

# Chemical Engineering Journal

## Activated sodium percarbonate-ozone (SPC/O<sub>3</sub>) hybrid hydrodynamic cavitation system for advanced oxidation processes (AOPs) of 1,4-dioxane in water.

--Manuscript Draft--

<b>Manuscript Number:</b>	CEJ-D-22-18851R2
<b>Article Type:</b>	Research Paper
<b>Keywords:</b>	Percarbonate; Wastewater Treatment; Ozonation; reactive oxygen species; Process intensification; Emerging organic pollutants EOCs
<b>Corresponding Author:</b>	Grzegorz Boczkaj, PhD.Sc.Eng. Gdansk University of Technology: Politechnika Gdanska Gdansk, POLAND
<b>First Author:</b>	Kirill Fedorov
<b>Order of Authors:</b>	Kirill Fedorov Manoj P. Rayaroth Noor S. Shah Grzegorz Boczkaj, PhD.Sc.Eng.
<b>Abstract:</b>	<p>Hydrodynamic cavitation (HC) was employed to activate sodium percarbonate (SPC) and ozone (O<sub>3</sub>) to degrade recalcitrant 1,4-dioxane. The degradation efficiency &gt;99% with a rate constant of <math>4.04 \times 10^{-2} \text{ min}^{-1}</math> was achieved in 120 min under the optimal conditions of cavitation number (<math>C_v</math>) 0.27, pH 5, molar ratio of oxidant to pollutant (rox) 8, ozone dose of 0.86 g h<sup>-1</sup> under 25±2 °C with initial concentration of 1,4-dioxane 100 ppm. The application of HC with SPC/O<sub>3</sub> increased the degradation efficiency by 43.32% in 120 min, confirming a synergistic effect between the coupled processes. In addition, the degradation efficiency of 1,4-dioxane in HC/SPC/O<sub>3</sub> was superior as compared to HC/H<sub>2</sub>O<sub>2</sub>/O<sub>3</sub>, suggesting that the presence of SPC has a significant role in degradation of 1,4-dioxane. Radical quenching experiment revealed highest contribution of hydroxyl (HO•) radicals in the degradation of 1,4-dioxane among carbonate (CO<sub>3</sub><sup>-</sup>) and superoxide (O<sub>2</sub><sup>-</sup>) radicals. The presence of co-existing anions resulted in an inhibitory effect in the following order: SO<sub>4</sub><sup>2-</sup> &gt; NO<sub>3</sub><sup>-</sup> &gt; Cl<sup>-</sup>. Based on GC-MS analysis, ethylene glycol diformate (EGDF) was detected as the main degradation product of 1,4-dioxane. The observed intermediate supports the radical route of 1,4-dioxane oxidation, which involves H-abstraction, ΔC-C splitting at the α-C position, subsequent dimerization, fragmentation and mineralization. Electric energy per order (EEO) for best process was 102.65 kWh-m<sup>3</sup>-order<sup>-1</sup>. Total cost of treatment was estimated as approx. 24 USD/m<sup>3</sup>. These findings confirmed the SPC as an efficient, environmentally-friendly alternative to H<sub>2</sub>O<sub>2</sub> and broadened the scope of HC-based AOPs for water and wastewater treatment.</p>
<b>Response to Reviewers:</b>	<p>Reviewer #2</p> <p>1. The authors have tried to address some problems raised in the previous comments. Nevertheless, one issue remains to be clarified before the manuscript can be considered for publication. The energy consumption (EEO) reported in Table 9 needs to be carefully checked. EEO refers to the energy demand for abating the concentration of a compound, not TOC, by 1 order in 1 m<sup>3</sup> water. The EEO for E-peroxone and photoelectron-peroxone reported in Table 9 is about 3-5 orders of magnitude higher than the values reported for these processes in literature, for example, Li et al., 2021; Yao et al., 2018; Yao et al., 2016. There must be something wrong in the calculations, which should be clarified. Therefore, a minor revision is required for the present manuscript.:</p> <p>Response: Thank you for pointing this out and literature provided. We apologize that our previously presented data were incorrect and we agree with your suggestion. We tried to estimate EEO values for processes available in the literature, however in some cases there were limited data.</p> <p>Therefore, we have revised the data presented in Table 9. The EEO values of electro-peroxone and photo-electro-peroxone were calculated in accordance with the equation</p>

provided by Wang et. al., [1] using rate constant of 1,4-dioxane degradation and assuming the average cell voltage as 7.8 V [2]. Obtained values along with corresponding references were indicated in discussion and the calculation was shown in Supplementary data.  
Corresponding comments on this aspect were provided in revised version of manuscript.

References:

[1]H. Wang, J. Zhan, L. Gao, G. Yu, S. Komarneni, Y. Wang, Kinetics and mechanism of thiamethoxam abatement by ozonation and ozone-based advanced oxidation processes, *J. Hazard. Mater.* 390 (2020) 122180.  
doi:10.1016/J.JHAZMAT.2020.122180.

[2]H. Wang, S. Yuan, J. Zhan, Y. Wang, G. Yu, S. Deng, J. Huang, B. Wang, Mechanisms of enhanced total organic carbon elimination from oxalic acid solutions by electro-peroxone process, *Water Res.* 80 (2015) 20–29.  
doi:10.1016/J.WATRES.2015.05.024.



FACULTY OF CIVIL  
AND ENVIRONMENTAL  
ENGINEERING

**COVER LETTER FOR SUBMISSION OF REVISED MANUSCRIPT**  
**Activated sodium percarbonate-ozone (SPC/O<sub>3</sub>) hybrid hydrodynamic cavitation system**  
**for advanced oxidation processes (AOPs) of 1,4-dioxane in water**

Subject: **SUBMISSION OF A REVISED MANUSCRIPT FOR EVALUATION**

**Dear prof. Kusic,**

We are enclosing herewith a revised manuscript entitled "*Activated sodium percarbonate-ozone (SPC/O<sub>3</sub>) hybrid hydrodynamic cavitation system for advanced oxidation processes (AOPs) of 1,4-dioxane in water*".

All of the suggestions raised by the Editor and Reviewer were thoroughly considered and adapted in the paper. We hope that the Reviewer will be satisfied.

With the submission of this manuscript we certify that the above-mentioned manuscript has not been published elsewhere, accepted for publication elsewhere or under editorial review for publication elsewhere

Sincerely yours,



*Corresponding author*

*Prof. Grzegorz Boczkaj, PhD. Sc. Eng.*

*Gdansk University of Technology*

Title: Activated sodium percarbonate-ozone (SPC/O<sub>3</sub>) hybrid hydrodynamic cavitation system for advanced oxidation processes (AOPs) of 1,4-dioxane in water  
MS No.: CEJ-D-22-18851 in: Chemical Engineering Journal

Reviewer #2

1. *The authors have tried to address some problems raised in the previous comments. Nevertheless, one issue remains to be clarified before the manuscript can be considered for publication. The energy consumption (EEO) reported in Table 9 needs to be carefully checked. EEO refers to the energy demand for abating the concentration of a compound, not TOC, by 1 order in 1 m<sup>3</sup> water. The EEO for E-peroxone and photoelectron-peroxone reported in Table 9 is about 3-5 orders of magnitude higher than the values reported for these processes in literature, for example, Li et al., 2021; Yao et al., 2018; Yao et al., 2016. There must be something wrong in the calculations, which should be clarified. Therefore, a minor revision is required for the present manuscript.:*

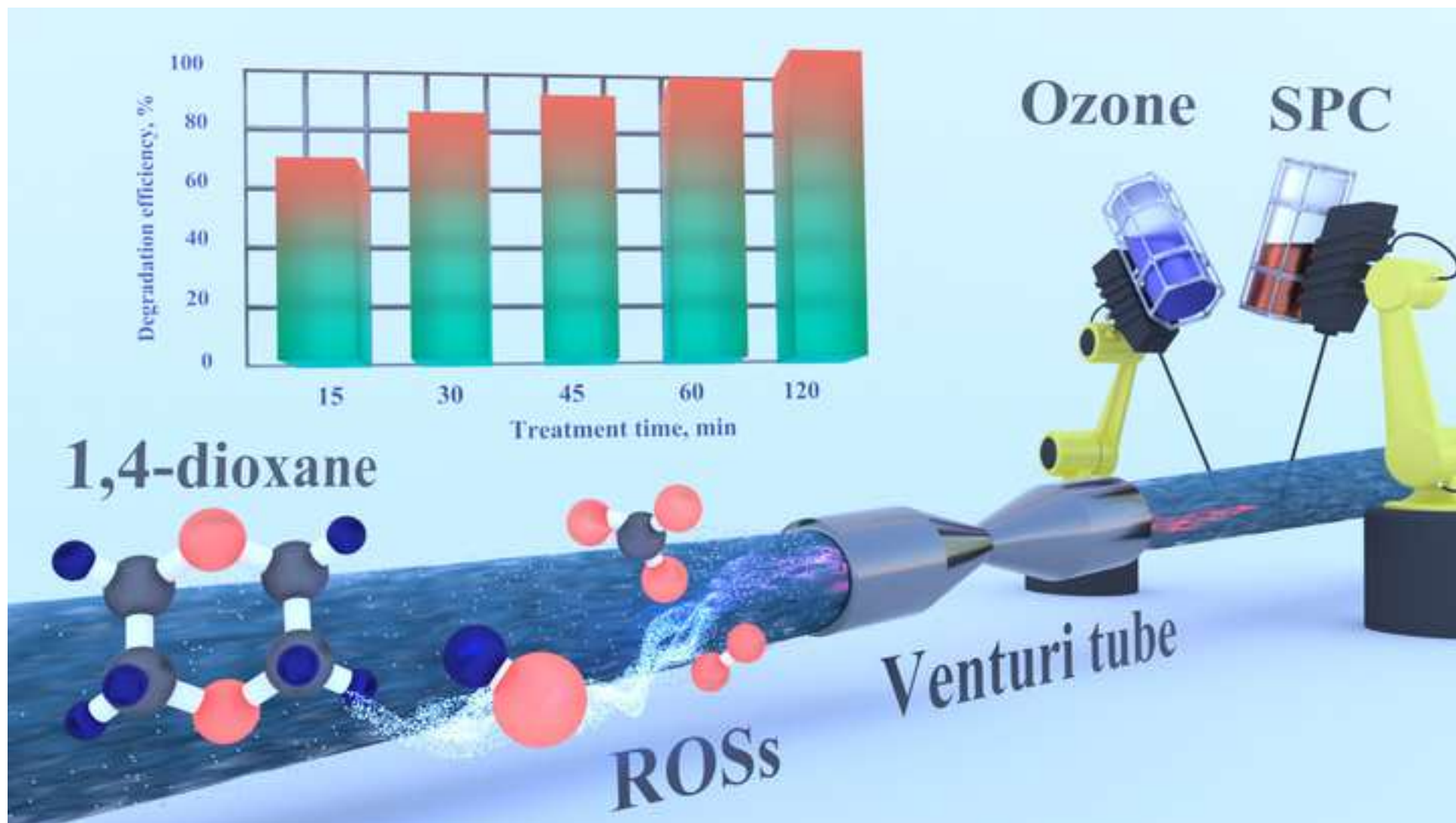
**Response:** Thank you for pointing this out and literature provided. We apologize that our previously presented data were incorrect and we agree with your suggestion. We tried to estimate EEO values for processes available in the literature, however in some cases there were limited data.

Therefore, we have revised the data presented in Table 9. The E<sub>EO</sub> values of electro-peroxone and photo-electro-peroxone were calculated in accordance with the equation provided by Wang et. al., [1] using rate constant of 1,4-dioxane degradation and assuming the average cell voltage as 7.8 V [2]. Obtained values along with corresponding references were indicated in discussion and the calculation was shown in Supplementary data.

Corresponding comments on this aspect were provided in revised version of manuscript.

References:

- [1] H. Wang, J. Zhan, L. Gao, G. Yu, S. Komarneni, Y. Wang, Kinetics and mechanism of thiamethoxam abatement by ozonation and ozone-based advanced oxidation processes, *J. Hazard. Mater.* 390 (2020) 122180. doi:10.1016/J.JHAZMAT.2020.122180.
- [2] H. Wang, S. Yuan, J. Zhan, Y. Wang, G. Yu, S. Deng, J. Huang, B. Wang, Mechanisms of enhanced total organic carbon elimination from oxalic acid solutions by electro-peroxone process, *Water Res.* 80 (2015) 20–29. doi:10.1016/J.WATRES.2015.05.024.



## Highlights

- Synergistic HC/SPC/O<sub>3</sub> process for degradation of emerging environmental pollutants
- Superior performance of HC/SPC/O<sub>3</sub> comparing to HC/H<sub>2</sub>O<sub>2</sub>/O<sub>3</sub>
- Improvement of sustainability and process safety of AOPs by percarbonate oxidant
- Green advanced oxidation based on cavitation phenomenon
- Importance of hydrodynamic cavitation in activation of oxidants

**Activated sodium percarbonate-ozone (SPC/O<sub>3</sub>) hybrid hydrodynamic cavitation system for advanced oxidation processes (AOPs) of 1,4-dioxane in water.**

Kirill Fedorov<sup>1</sup>, Manoj P. Rayaroth<sup>2</sup>, Noor S. Shah<sup>3</sup>, Grzegorz Boczkaj<sup>1,4,\*</sup>

<sup>1</sup>*Gdańsk University of Technology, Faculty of Civil and Environmental Engineering, Department of Sanitary Engineering, 80-233 Gdańsk, G. Narutowicza 11/12 Str, Poland.*

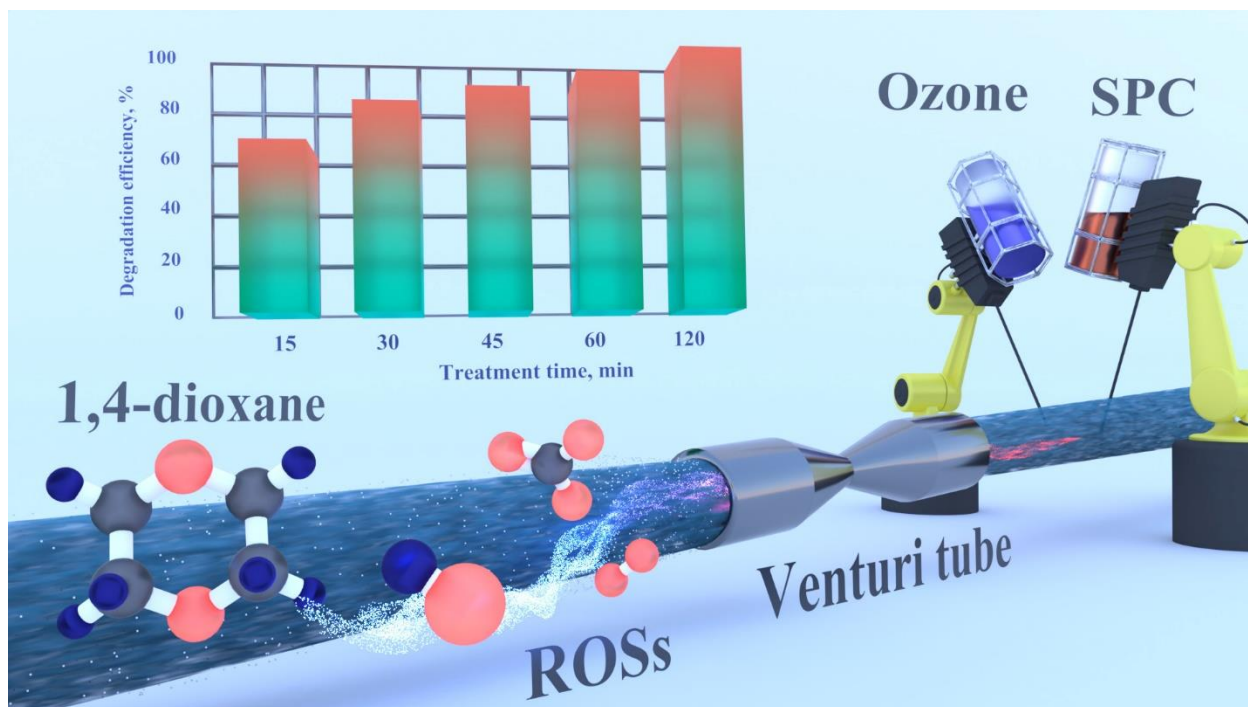
<sup>2</sup>*GREMI, UMR 7344, Université d'Orléans, CNRS, 45067 Orléans, France.*

<sup>3</sup>*Department of Environmental Sciences, COMSATS University Islamabad, Vehari Campus 61100, Pakistan.*

<sup>4</sup>*EkoTech Center, Gdansk University of Technology, G. Narutowicza St. 11/12, 80-233 Gdansk, Poland.*

*\* Corresponding author: Dr Grzegorz Boczkaj, Assoc. Prof., PhD. Sc. Eng. Gdansk University of Technology, Faculty of Civil and Environmental Engineering, Department of Sanitary Engineering, 80 – 233 Gdansk, G. Narutowicza St. 11/12, Poland. Fax: (+48 58) 347-26-94; Tel: (+48) 697970303; E-mail: [grzegorz.boczkaj@pg.edu.pl](mailto:grzegorz.boczkaj@pg.edu.pl) or [grzegorz.boczkaj@gmail.com](mailto:grzegorz.boczkaj@gmail.com)*

## Graphical abstract





## 1 Abstract

2 Hydrodynamic cavitation (HC) was employed to activate sodium percarbonate (SPC) and ozone (O<sub>3</sub>) to  
3 degrade recalcitrant 1,4-dioxane. The degradation efficiency >99% with a rate constant of  $4.04 \times 10^{-2} \text{ min}^{-1}$   
4 was achieved in 120 min under the optimal conditions of cavitation number (C<sub>v</sub>) 0.27, pH 5, molar ratio  
5 of oxidant to pollutant ( $r_{ox}$ ) 8, ozone dose of  $0.86 \text{ g h}^{-1}$  under  $25 \pm 2 \text{ }^\circ\text{C}$  with initial concentration of 1,4-  
6 dioxane 100 ppm. The application of HC with SPC/O<sub>3</sub> increased the degradation efficiency by 43.32% in  
7 120 min, confirming a synergistic effect between the coupled processes. In addition, the degradation  
8 efficiency of 1,4-dioxane in HC/SPC/O<sub>3</sub> was superior as compared to HC/H<sub>2</sub>O<sub>2</sub>/O<sub>3</sub>, suggesting that the  
9 presence of SPC has a significant role in degradation of 1,4-dioxane. Radical quenching experiment  
10 revealed highest contribution of hydroxyl (HO<sup>•</sup>) radicals in the degradation of 1,4-dioxane among  
11 carbonate (CO<sub>3</sub><sup>•-</sup>) and superoxide (O<sub>2</sub><sup>•-</sup>) radicals. The presence of co-existing anions resulted in an  
12 inhibitory effect in the following order: SO<sub>4</sub><sup>2-</sup> > NO<sub>3</sub><sup>-</sup> > Cl<sup>-</sup>. Based on GC-MS analysis, ethylene glycol  
13 diformate (EGDF) was detected as the main degradation product of 1,4-dioxane. The observed  
14 intermediate supports the radical route of 1,4-dioxane oxidation, which involves H-abstraction, ΔC-C  
15 splitting at the α-C position, subsequent dimerization, fragmentation and mineralization. Electric energy  
16 per order (E<sub>EO</sub>) for best process was  $176,79 \text{ kWh} \cdot \text{m}^{-3} \cdot \text{order}^{-1}$ . Total cost of treatment was estimated as  
17 approx. 20 USD/m<sup>3</sup>. These findings confirmed the SPC as an efficient, environmentally-friendly  
18 alternative to H<sub>2</sub>O<sub>2</sub> and broadened the scope of HC-based AOPs for water and wastewater treatment.

19 Keywords: percarbonate; wastewater treatment; ozonation; reactive oxygen species; process  
20 intensification; Emerging organic pollutants EOCs.

21

22

23

24



## 25 1. Introduction

26

27 1,4-dioxane also named as 1,4-diethylene oxide, an important stabilizer of chlorinated solvents has found  
28 a wide variety of industrial applications such as aerosol additive, wetting and dispersing agent. It is also  
29 formed during the production of surfactants and synthesis of poly(ethylene) terephthalate [1]. The  
30 occurrence of 1,4-dioxane has been detected in municipal water supply, landfill leachate and  
31 groundwaters [2,3]. Such widespread occurrence of 1,4-dioxane is mainly originated due to the improper  
32 disposal of the effluents, resistance of 1,4-dioxane to biodegradation and merely complete miscibility  
33 with water. In terms of toxicity, 1,4-dioxane has been shown carcinogenic to animals and classified as  
34 potentially (Class B2) carcinogenic to human by the United States Environmental Protection Agency  
35 [1,4]. In connection with this, stringent water quality standards regulating the concentration of 1,4-  
36 dioxane in water have been adopted to reduce the health risk. However, the conventional water treatment  
37 methods based on biodegradation were found ineffective towards 1,4-dioxane [5–7]. Therefore,  
38 tremendous efforts have been devoted for the development of technologies to degrade 1,4-dioxane in  
39 water. Among the tested technologies, advanced oxidation processes (AOPs) based on the generation of  
40 highly reactive radical species appeared to be promising green technologies for remediation of 1,4-  
41 dioxane from aqueous environment [5,8–11].

42 As a part of AOPs,  $\text{H}_2\text{O}_2$  produces hydroxyl ( $\text{HO}^\bullet$ ) radicals with an extremely strong oxidation capacity  
43 ( $E^0$  2.8 V), which can allow to achieve complete mineralization of treated organic pollutants [12]. The  
44 production of  $\text{HO}^\bullet$  radicals is generally proceeded through the combination of  $\text{H}_2\text{O}_2$  with oxidants (PS,  
45 PMS), catalysts ( $\text{Fe}^{2+}$ ,  $\text{TiO}_2$ ) or energy input (ultrasound, UV-irradiation). Among the combined  
46 processes,  $\text{H}_2\text{O}_2/\text{O}_3$  is a well-known and powerful method denominated as peroxone, which involves  
47 direct and indirect oxidation of pollutants. The effectiveness of  $\text{H}_2\text{O}_2/\text{O}_3$  has been proven towards the  
48 degradation of 1,4-dioxane [6,13], dyes [14], pharmaceuticals [15,16], volatile organic compounds  
49 (VOCs) [17] and wastewaters [18,19]. In peroxone process,  $\text{HO}^\bullet$  radicals are generated *via* the accelerated  
50 decomposition of  $\text{O}_3$  initiated by  $\text{H}_2\text{O}_2$  and alternative activation of  $\text{H}_2\text{O}_2$  by  $\text{O}_3$ . Nevertheless, the use of  
51  $\text{H}_2\text{O}_2$  is associated with serious safety concerns related with a risk of explosion during the transportation  
52 and corrosion of equipment. Moreover, the application of  $\text{H}_2\text{O}_2$  in AOPs is commonly related with self-

53 scavenging or radical recombination reactions raising the issue of H<sub>2</sub>O<sub>2</sub> dosage and introduction mode  
54 optimization.

55 Recently, studies on H<sub>2</sub>O<sub>2</sub>-based AOPs are focused on sodium percarbonate (SPC), namely Na<sub>2</sub>CO<sub>3</sub> ×  
56 1.5H<sub>2</sub>O<sub>2</sub> as a safe and cheap alternative to H<sub>2</sub>O<sub>2</sub>. Besides, this trend is reasoned with a number of  
57 advantages such as prevention of acidification of treated media and wide operating pH range [20,21].  
58 Attempts on SPC activation have been made using Fe<sup>2+</sup> [22–24], graphene oxide [25], protonated g-C<sub>3</sub>N<sub>4</sub>  
59 [26], zero valent iron (ZVI) [27], vanadium (IV) [28], UV [29] and ultrasound [21]. Unlike H<sub>2</sub>O<sub>2</sub>, the  
60 oxidation capacity of SPC-based AOPs is conditioned by a variety of ROS, including superoxide (O<sub>2</sub><sup>•-</sup>)  
61 and carbonate (CO<sub>3</sub><sup>•-</sup>) radicals. The latter is generated through the consumption of HO<sup>•</sup> radicals and  
62 exhibit lower oxidation potential of 1.78 V at pH 7 [30]. In spite of this, CO<sub>3</sub><sup>•-</sup> radicals selectively react  
63 with organic pollutants containing electron rich functional groups. For instance, as an electron acceptor  
64 CO<sub>3</sub><sup>•-</sup> radical rapidly reacts with *p*-substituted phenols and anilines with a rate constant of 10<sup>7</sup>-10<sup>8</sup> M<sup>-1</sup> s<sup>-1</sup>  
65 and 10<sup>5</sup>-10<sup>7</sup> M<sup>-1</sup> s<sup>-1</sup>, respectively [31–33]. Moreover, the concentration of CO<sub>3</sub><sup>•-</sup> radicals in sunlit surface  
66 water appeared to be two orders of magnitude higher than HO<sup>•</sup> radicals under the same conditions [34].  
67 Therefore, SPC-based AOPs are seemed to be a preferable option for the degradation of organic  
68 pollutants bearing electron rich moieties and, particularly, 1,4-dioxane.

69 Although, AOPs are considered as effective and environmentally friendly techniques for the degradation  
70 organic contaminants, the industrial implementation of AOPs in water treatment schemes is hindered. To  
71 achieve a satisfactory level of degradation, the application of traditional AOPs require high operational  
72 cost due to large consumption of oxidants and energy [35]. In the light of this, a recent trend on  
73 integration of AOPs with cavitation is a promising route for the improvement of AOPs. The development  
74 of hybrid processes based on cavitation and AOPs showed encouraging results anticipating the  
75 implementation of novel technologies in water/wastewater treatment [36–39]. Cavitation is an emerging  
76 technique which is often employed to improve the effectiveness of AOPs. The key mechanism relying  
77 behind the cavitation phenomenon relate to the formation, growth and violent collapse of cavitation  
78 bubbles. Since, the collapse of bubbles releases a large magnitude of energy in a short time interval,  
79 regions of extreme conditions or so-called “hot spots” are created. Such conditions are capable to form  
80 radical species through to the pyrolytic disassociation of water or proceed the activation of H<sub>2</sub>O<sub>2</sub>, O<sub>3</sub> and  
81 other peroxides. Owing to the continuous flow operation, high cavitational yield and effectiveness

82 towards the degradation of pollutants, hydrodynamic cavitation has a great potential for scale up and  
83 application in real wastewater treatment systems [40–42]. Herein, this study was performed with the  
84 following objectives: i). to investigate the degradation of 1,4-dioxane in SPC/O<sub>3</sub> process under  
85 hydrodynamic cavitation (HC); ii). to understand the synergy in HC/SPC/O<sub>3</sub> the degradation kinetics of  
86 1,4-dioxane in sole and coupled processes; iii). to identify the reactive species in HC/SPC/O<sub>3</sub> by  
87 quenching experiments using specific radical scavengers; iv). to perform the degradation under  
88 environmental relevant conditions varying pH and in the presence of inorganic anions; and finally, v). to  
89 identify the transformation products and elucidate the mechanism of 1,4-dioxane degradation in  
90 HC/SPC/O<sub>3</sub>.

91

## 92 **2. Materials and methods**

93

### 94 *2.1 Chemicals*

95

96 1,4-dioxane (reagent grade, p.a., 99%), sodium nitrate (pure), sodium hydroxide (pure p.a., 98.8%),  
97 chloroform (pure p.a.), acetone, dichloromethane, 2-propanol (pure p.a.), hydrogen peroxide (pure p.a.,  
98 30%), potassium iodide (pure p.a.) and sodium thiosulfate pentahydrate (acs pure p.a.) were purchased  
99 from POCH (Poland). Sodium percarbonate (avail. H<sub>2</sub>O<sub>2</sub> 20-30%), cyclohexanone and phenol were  
100 purchased from Sigma-Aldrich (Germany). Sodium sulfate (anhydrous, pure, p.a.), sodium carbonate  
101 (anhydrous, pure p.a.), sodium azide (pure p.a.) and sulfuric acid (pure p.a., 95%) were purchased from  
102 Chempur (Poland). Sodium chloride (pure) was purchased from Stanlab (Poland) and 1,4-benzoquinone  
103 (99%) was purchased from Acros Organics (Belgium). All chemicals and solvents were of analytical  
104 grade and were used as received without purification. Ultrapure quality water (18.2 MΩcm<sup>-1</sup>) from  
105 Millipore<sup>®</sup> system (Direct-Q UV-R model) was used for preparation of reaction solution.

106

### 107 *2.2 Experimental procedure*

108

109 The degradation experiments of 1,4-dioxane were conducted in a hydrodynamic cavitation reactor with  
110 close-circuit system (Supplementary data, **Fig. S1**). The reactor was composed of feed tank equipped with

111 a mechanical stirrer, temperature indicator and water condenser to maintain the reaction temperature.  
112 Sequential pumping system (MS 801-4, 1360 min<sup>-1</sup>, TECHTOP® MOTOR, Shanghai, China) connected  
113 with electromagnetic flowmeter (MPP 600 by MAGFLO®) was used to circulate water through the  
114 cavitating device and by-pass line. The cavitating device consisted of brass Venturi tube with 2-mm ID of  
115 the throat section. Digital manometers (Suku, Germany) were mounted on the upstream and downstream  
116 lines of Venturi tube to measure the pressure. Polytetrafluoroethylene (PTFE) pipes and stainless-steel  
117 joints were used to connect the units. In a typical experimental procedure, 5 L of model solution  
118 containing 100 ppm of 1,4-dioxane was added in the feed tank and treated for 120 min at 20±2 °C.  
119 Sample aliquots of 20 mL were collected at regular time interval. The SPC solution was injected through  
120 the port with inner porous membrane to attain the required molar ratio of SPC to 1,4-dioxane. Dry air  
121 with a certain flow rate was connected to a Tytan 32 (Erem, Poland) ozone generator to purge ozone to  
122 the upstream line of Venturi tube. All experiments were performed in duplicate and experimental errors  
123 were within 5%.

### 124 2.3 Analysis

125 Prior to GC analyses, dispersive liquid-liquid microextraction (DLLME) was employed to extract 1,4-  
126 dioxane from water samples. The procedure of DLLME was as follows: 5 µL of internal standard  
127 (cyclohexanone) were added to 10 mL of samples. Then 0.9 mL mixture of dispersing and extraction  
128 solvent composed of dichloromethane and acetone (50:40). After 1 min shaking, the samples were  
129 centrifugated for 10 min at 5000 rpm (EBA 8S, Hettich, Germany). A 300 µL of organic phase were  
130 extracted and placed in glass conical inserts for analysis [9,43].

131 A quantitative analysis of 1,4-dioxane concentration was studied using a Clarus 500 (Perkin Elmer, USA)  
132 gas chromatograph equipped with flame ionization detector (GC-FID). A capillary column (60 m × 0.32  
133 mm ID, 1.8 µm DB624, Agilent, USA) was used is separations. Parameters setting of GC-FID were as  
134 follows: temperature program - 50 °C (5 min) ramped at 10 °C/min to 275 °C (5 min), detector  
135 temperature 275 °C. A nitrogen was used as carrier gas with volumetric flowrate of 5 mL/min. Detector  
136 gases flow rate: air 450 mL/min, hydrogen 40 mL/min.

137 The identification of 1,4-dioxane degradation products was performed using a GCMSQP2010SE  
138 (Shimadzu, Japan) gas chromatograph (GC) coupled to a mass spectrometer (MS). A capillary column  
139 (100 m × 0.2 mm ID, 0.1 µm DHA, Restek, USA) was used for separation of analytes. A hydrogen

140 (supplied from PGX500 hydrogen generator, Perkin Elmer, USA) was used as carrier gas (1 mL/min),  
141 injection port temperature was 300 °C and GC-MS transfer line temperature was 310 °C. The oven  
142 temperature program was 40 °C (isothermal for 5 min) ramped at 5 °C/min to 220 °C. Ion source (EI, 70  
143 eV) temperature was 200 °C. A mass-to-charge ratio of 34 to 220 m/z was selected for SCAN mode  
144 analysis of byproducts.

145 The concentration of O<sub>3</sub> in introduced gaseous oxidant stream was measured by iodometric titration  
146 method. The experimental setup consisted of ozone generator (Erem 32, Poland) and two connected gas  
147 washing bottles in series. Each bottle was filled with 400 mL of acidified (pH 3) KI (2% w/w) solution to  
148 trap O<sub>3</sub>. The compressed dry air containing O<sub>3</sub> was bubbled through KI solution using a sintered glass  
149 disc located in the bottom half of bottles. A standardized 0.001 N Na<sub>2</sub>S<sub>2</sub>O<sub>3</sub> solution was used as a titrant  
150 and 5% (w/v) starch solution as an indicator. The dose of O<sub>3</sub> at carrier gas flow rate of 0.5, 1.0, 1.5, 2.0  
151 and 2.5 L min<sup>-1</sup> were determined as 0.23, 0.40, 0.74, 0.86 and 0.94 g h<sup>-1</sup>, respectively. The content of total  
152 organic carbon (TOC) was measured using TOC-LCSH instrument (Shimadzu, Japan). All tubing  
153 connecting ozone generator with HC reactor and gas absorption bottles were made of PTFE (Teflon).

### 154 **3. Results and discussion**

#### 155 *3.1 Effect of cavitation number*

156 Cavitation conditions (e.g., size of cavitation bubbles, dynamics) are defined by the factors, such as a  
157 geometry of the cavitating device, flow velocity, temperature, content of dissolved gases and suspended  
158 particles. The intensity of cavitation directly depends on the turbulence intensity of the liquid and number  
159 of generated cavities. The turbulence intensity, in turn, is related to geometry of the cavitating device and  
160 flow conditions of the liquid [44]. The relation between flow conditions and the cavitation intensity can  
161 be defined using cavitation number (C<sub>v</sub>). Thus, the determination of optimal C<sub>v</sub> is required for the  
162 regulation of flow conditions to get max cavitation events and can be expressed as follows [45–47]:

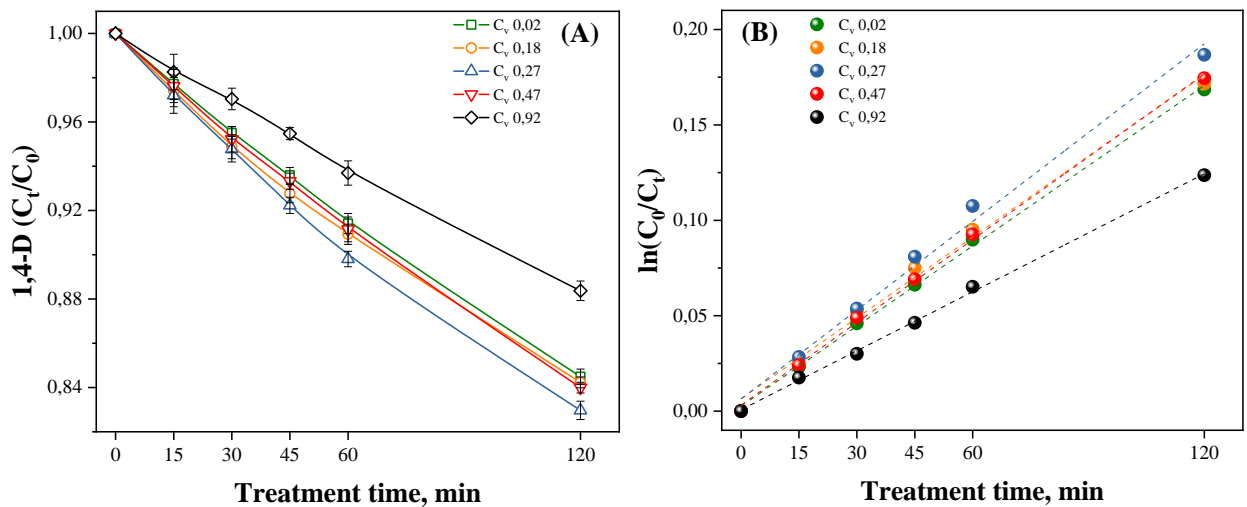
$$163 \quad C_v = \frac{p_2 - p_v}{\frac{1}{2}u_0^2 \rho}, \quad (1)$$

164 where, p<sub>2</sub> is the recovered downstream pressure, p<sub>v</sub> – vapor pressure of the liquid, u<sub>0</sub> is liquid linear  
165 velocity at the throat of cavitating constriction and ρ is the density of the treated liquid.

166 In this study, the effectiveness of sole HC towards 1,4-dioxane degradation was performed varying the  
 167 liquid velocity to determine the optimal  $C_v$ . All studies in this paper were performed for primary  
 168 concentration of dioxane 100 ppms. This concentration was selected to address effectiveness of studied  
 169 processes to concentration level that can be expected in the industrial effluents. Dioxane is well soluble in  
 170 water. Concentration values much higher than 100 ppms, are not expected, as in such case simple  
 171 purification processes based on adsorption or membrane treatment would be effectively used. Pseudo-  
 172 first-order model with regard to the concentration of 1,4-dioxane was employed to depict the degradation  
 173 kinetics (Eq. 2).

$$174 \quad \ln \frac{C_0}{C_t} = kt, \quad (2)$$

175 where  $C_0$  and  $C_t$  are initial and instant concentration of 1,4-dioxane, respectively,  $k$  represents the  
 176 degradation rate constant and  $t$  is the treatment time. The rate constant of each process was calculated by  
 177 plotting  $\ln(C_0/C_t)$  against time of treatment.



178 **Figure 1.** Effect of  $C_v$  on the degradation 1,4-dioxane in sole HC: (a) degradation efficiency, (b) pseudo-  
 179 first-order kinetic plots ( $[1,4-D]_0$  100 ppm, pH<sub>0</sub> 5,  $20 \pm 2$  °C).

181 As depicted in **Fig. 1a**, the percent degradation of 1,4-dioxane was 11.63, 16.01 and 17.03% for  $C_v$  0.92,  
 182 0.47 to 0.27, respectively. The degradation rate constant was increased from  $1.03 \times 10^{-3} \text{ min}^{-1}$  to  $1.43 \times$   
 183  $10^{-3} \text{ min}^{-1}$  (**Table 1**) with a reduction of  $C_v$  from 0.92 to 0.27. These observations indicated that the  
 184 increase of the liquid velocity and, subsequently, inlet pressure, increased the cavitation intensity, which  
 185 is reflected in higher degradation of 1,4-dioxane. However, the continuous reduction of  $C_v$  to 0.18 and

186 0.02 resulted in 15.76 and 15.51% of 1,4-dioxane degradation, respectively. The rate constants of 1,4-  
 187 dioxane degradation using  $C_v$  0.18 and 0.02 were  $1.41 \times 10^{-3}$  and  $1.40 \times 10^{-3} \text{ min}^{-1}$ , respectively. Similar  
 188 findings were extensively reported and attributed due to supercavitation or so-called choked cavitation,  
 189 which occurs beyond the critical level of inlet pressure in Venturi tube. In choked cavitation, a large  
 190 number of generated cavities undergo mutual coalescence yielding a vaporous cavity cloud with reduced  
 191 collapse pressure [39,44]. Based on the obtained results, 0.27 was selected as the optimal  $C_v$  for the rest  
 192 of experiments.

193 **Table 1.** Kinetic parameters of 1,4-dioxane degradation in sole HC at different  $C_v$ .

	Cavitation number ( $C_v$ )				
	0.02	0.18	0.27	0.47	0.92
$k \times 10^{-2}, \text{ min}^{-1}$	0.140	0.141	0.155	0.145	0.103
$R^2$	0.998	0.993	0.992	0.998	0.999

194

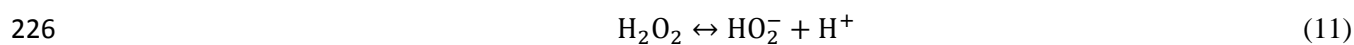
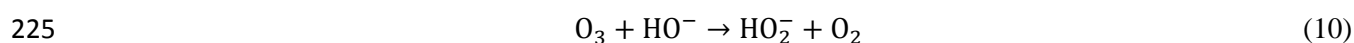
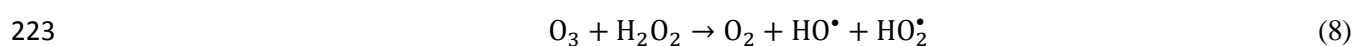
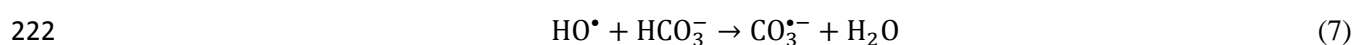
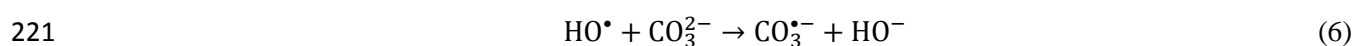
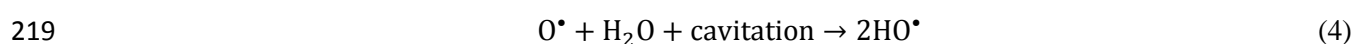
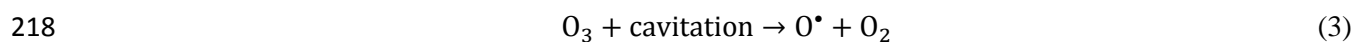
### 195 3.2 Enhanced degradation of 1,4-dioxane by HC/SPC/O<sub>3</sub>

196

197 The degradation efficiency of HC/O<sub>2</sub>, HC/O<sub>3</sub>, HC/SPC, SPC/O<sub>3</sub> and HC/SPC/O<sub>3</sub> towards 1,4-dioxane was  
 198 examined and depicted in **Fig. 2a**. According to **Fig. 2a**, 18.29% of 1,4-dioxane was degraded in 120 min,  
 199 showing higher degradation efficiency than sole HC. This can be explained by formation of additional  
 200 nuclei for the growth of cavitation bubbles as a gas is purged to the upstream line of Venturi tube.  
 201 Furthermore, about 24.34 and 22.76% of 1,4-dioxane degradation were obtained within 120 min in  
 202 HC/O<sub>3</sub> and HC/SPC, respectively. These observations indicate the increase of number of reactive radicals  
 203 produced in the presence of oxidants according to **Eqs. 3-7** [20,40,48,49]. The generation of radicals was  
 204 increased further and reflected in 56.02% of 1,4-dioxane degradation in 120 min as O<sub>3</sub> was combined  
 205 with SPC in the absence of HC. Although, the radicals in SPC/O<sub>3</sub> are produced according to peroxone  
 206 process as shown in **Eqs. 8, 9** [45], the presence of SPC initiates chain reactions to yield radicals through  
 207 the decomposition of O<sub>3</sub> and H<sub>2</sub>O<sub>2</sub>. Particularly, alternative decomposition routes of O<sub>3</sub> and H<sub>2</sub>O<sub>2</sub> with  
 208 formation of HO<sub>2</sub><sup>-</sup> are occurred under the alkaline pH of SPC (**Eqs. 10, 11**) [45,50]. Obtained HO<sub>2</sub><sup>-</sup>  
 209 participate in a series of radical chain reactions and are eventually converted to highly reactive HO<sup>•</sup>  
 210 radicals. Coupling of HC with SPC/O<sub>3</sub> significantly increased the degradation efficiency of 1,4-dioxane  
 211 giving 99.34% in 120 min. The observed enhancement of 1,4-dioxane degradation in SPC/O<sub>3</sub> is

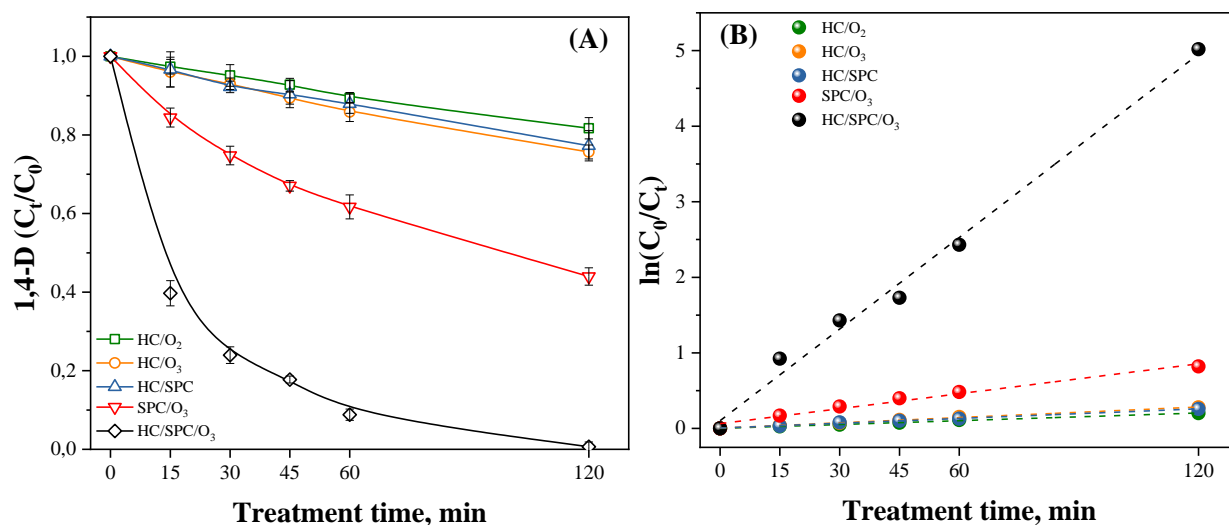


212 presumably attributed to the following beneficial factors provided by HC: i). thermal effect of so-called  
 213 “hot spots” due the adiabatic collapse of cavitation bubbles assisted the cleavage of chemical bonds  
 214 accelerating radical chain reactions; ii). continuous circulation along with shock waves improved the  
 215 utilization of O<sub>3</sub> and facilitated the overall mass transfer in the system; iii). owing to the extreme  
 216 conditions in “hot spots”, HC continuously produces radical species, thus, promoting the chain radical  
 217 reactions.



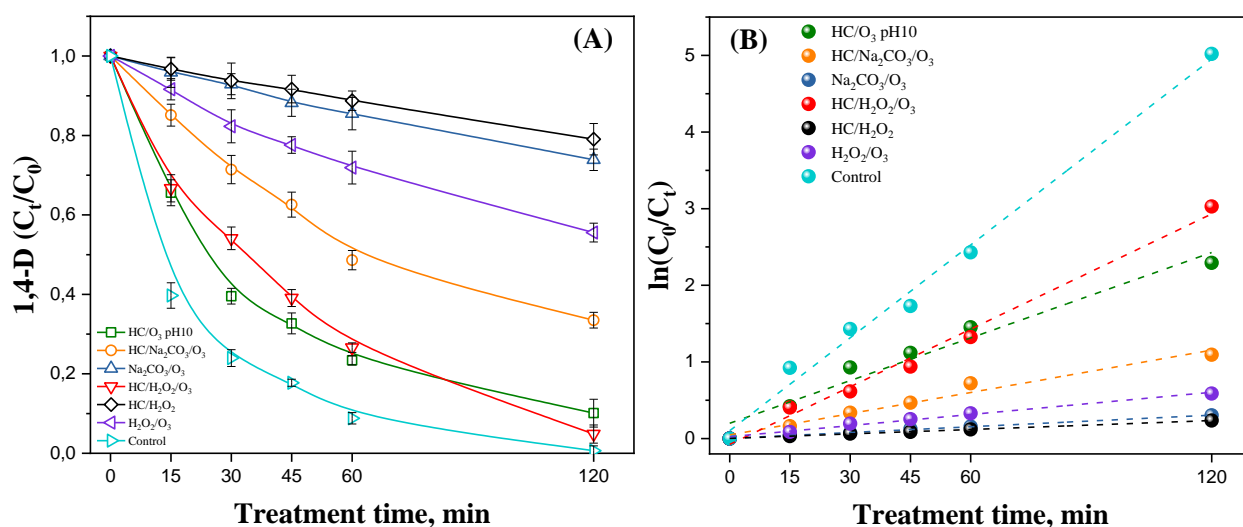
227 As shown in **Table 2**, the pseudo-first-order rate constant of 1,4-dioxane degradation HC/O<sub>2</sub>, HC/O<sub>3</sub>,  
 228 HC/SPC and SPC/O<sub>3</sub> were  $1.70 \times 10^{-3}$ ,  $2.32 \times 10^{-3}$ ,  $2.12 \times 10^{-3}$ ,  $6.60 \times 10^{-3} \text{ min}^{-1}$ , respectively, whereas  
 229 the *k* value in HC/SPC/O<sub>3</sub> was  $4.04 \times 10^{-2} \text{ min}^{-1}$ . Obtained *k* values demonstrate the distinct superiority of  
 230 the hybrid HC/SPC/O<sub>3</sub> over the binarily integrated processes in degradation of 1,4-dioxane. The  
 231 synergistic index ( $\xi$ ) of HC/SPC/O<sub>3</sub> calculated using *k* values according to **Eq. 12** was 4.32, which  
 232 indicates a remarkable synergy occurred in HC/SPC/O<sub>3</sub> in comparison with the cumulative effect of  
 233 individual processes. Although the value of  $\xi$  in HC/H<sub>2</sub>O<sub>2</sub>/O<sub>3</sub> was 3.83, the degradation efficiency of 1,4-  
 234 dioxane was 95.16% after 120 min, whereat the reaction constant was lower by  $1.54 \times 10^{-2} \text{ min}^{-1}$   
 235 compared to HC/SPC/O<sub>3</sub>.

$$\xi = \frac{k_{\text{HC/SPC/O}_3}}{k_{\text{SPC/O}_3} + k_{\text{HC}} + (k_{\text{HC/SPC}} - k_{\text{HC}}) + (k_{\text{HC/O}_3} - k_{\text{HC}})} \quad (12)$$



237

238 **Figure 2.** Effect of different processes on the degradation 1,4-D: (a) degradation efficiency, (b) pseudo-  
239 first-order kinetic plots ([1,4-D]<sub>0</sub> 100 ppm, C<sub>v</sub> 0.27, SPC *r*<sub>ox</sub> 8, [O<sub>3</sub>] 0.86 g h<sup>-1</sup>, pH<sub>0</sub> 5, 20±2 °C).



240

241 **Figure 3.** Effect of various processes on the degradation 1,4-D: (a) degradation efficiency, (b) pseudo-  
242 first-order kinetic plots ([1,4-D]<sub>0</sub> 100 ppm, C<sub>v</sub> 0.27, Na<sub>2</sub>CO<sub>3</sub>=H<sub>2</sub>O<sub>2</sub> *r*<sub>ox</sub> 8, [O<sub>3</sub>] 0.86 g h<sup>-1</sup>, 20±2 °C).

243 To further clarify the role of SPC in degradation of 1,4-dioxane by HC/SPC/O<sub>3</sub>, a series of additional  
244 experiments, including addition of sodium carbonate, have been conducted. As depicted in **Fig. 3a**,  
245 HC/Na<sub>2</sub>CO<sub>3</sub>/O<sub>3</sub> resulted in 66.50% of 1,4-dioxane degradation within 120 min, whereas it was only  
246 26.11% for O<sub>3</sub>/Na<sub>2</sub>CO<sub>3</sub> in the absence of HC, indicating a considerable contribution of HC in  
247 decomposition of O<sub>3</sub>. On the other hand, a discernable improve of 1,4-dioxane degradation was observed  
248 when comparing HC/Na<sub>2</sub>CO<sub>3</sub>/O<sub>3</sub> and Na<sub>2</sub>CO<sub>3</sub>/O<sub>3</sub> with corresponding HC/SPC/O<sub>3</sub> and SPC/O<sub>3</sub>. Thus, the

249 degradation efficiency of 1,4-dioxane in HC/Na<sub>2</sub>CO<sub>3</sub>/O<sub>3</sub> was lower by 32.84% compared to HC/SPC/O<sub>3</sub>,  
 250 while it was 29.91% for Na<sub>2</sub>CO<sub>3</sub>/O<sub>3</sub> and SPC/O<sub>3</sub>. Corresponding *k* values (**Table 2**) were increased from  
 251  $9.22 \times 10^{-3}$  to  $4.04 \times 10^{-2} \text{ min}^{-1}$  for HC/Na<sub>2</sub>CO<sub>3</sub>/O<sub>3</sub> and HC/SPC/O<sub>3</sub> and from  $2.52 \times 10^{-3}$  to  $6.60 \times 10^{-3}$   
 252  $\text{min}^{-1}$  for Na<sub>2</sub>CO<sub>3</sub>/O<sub>3</sub> and SPC/O<sub>3</sub>, respectively. In addition, application of H<sub>2</sub>O<sub>2</sub> in HC/O<sub>3</sub> improved the  
 253 degradation efficiency of 1,4-dioxane by 70.82% after 120 min. These results signify the essential role of  
 254 H<sub>2</sub>O<sub>2</sub> in formation of radical species in HC/SPC/O<sub>3</sub>. Nevertheless, the degradation efficiency attained by  
 255 HC/H<sub>2</sub>O<sub>2</sub>/O<sub>3</sub> was significantly lower than HC/SPC/O<sub>3</sub>. Similarly, the increase of pH to 10 in HC/O<sub>3</sub>  
 256 increased the degradation efficiency to 65.55%, due to the promoted O<sub>3</sub> decomposition, however, HC/O<sub>3</sub>  
 257 at pH 10 showed lower efficiency than HC/SPC/O<sub>3</sub>. Although, HCO<sub>3</sub><sup>-</sup> and CO<sub>3</sub><sup>2-</sup> anions are anticipated to  
 258 scavenge of HO<sup>•</sup> radicals (**Eqs. 6, 7**) and slowly react with 1,4-dioxane ( $\sim 10^5 \text{ M}^{-1} \text{ s}^{-1}$ ) [51–53], these  
 259 findings suggest, a partial participation of HCO<sub>3</sub><sup>-</sup> and CO<sub>3</sub><sup>-</sup> radicals in degradation of 1,4-dioxane.  
 260 Therefore, the contribution of HCO<sub>3</sub><sup>-</sup> and CO<sub>3</sub><sup>-</sup> radicals should be further clarified (detailed investigation  
 261 is presented in section 3.6).

262 **Table 2.** Kinetic parameters of 1,4-dioxane degradation in studied processes.

Type of process	<i>k</i> × 10 <sup>-2</sup> , min <sup>-1</sup>	R <sup>2</sup>
HC/O <sub>2</sub>	0.170	0.996
HC/H <sub>2</sub> O <sub>2</sub>	0.194	0.999
HC/SPC	0.212	0.995
HC/O <sub>3</sub>	0.232	0.997
Na <sub>2</sub> CO <sub>3</sub> /O <sub>3</sub>	0.252	0.998
H <sub>2</sub> O <sub>2</sub> /O <sub>3</sub> , pH10	0.483	0.991
SPC/O <sub>3</sub>	0.660	0.980
HC/Na <sub>2</sub> CO <sub>3</sub> /O <sub>3</sub>	0.922	0.973
HC/O <sub>3</sub> , pH10	1.857	0.963
HC/H <sub>2</sub> O <sub>2</sub> /O <sub>3</sub> , pH10	2.506	0.991
HC/SPC/O <sub>3</sub>	4.041	0.992

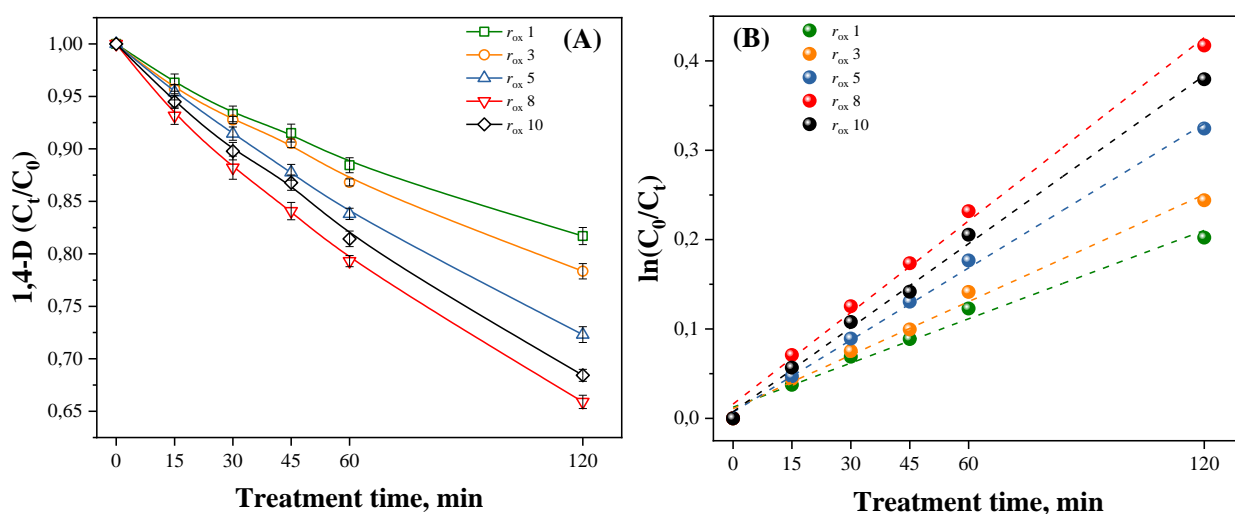
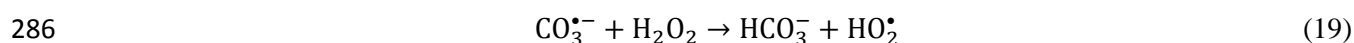
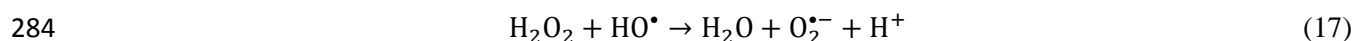
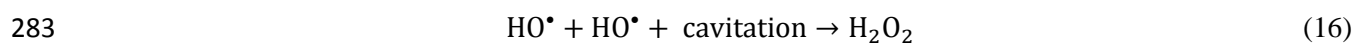
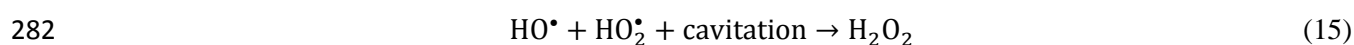
263

### 264 3.3 Effect of SPC dosage

265 Since SPC is a precursor of radical species, the dose of added SPC critically affects the effectiveness and  
 266 operational cost of HC/SPC/O<sub>3</sub>. In order to determine the optimal dosage of SPC, the degradation of 1,4-  
 267 dioxane was performed in HC/SPC with *r*<sub>ox</sub> ranging from 1 to 10, where the value of *r*<sub>ox</sub> represents the



268 molar ratio of SPC to 1,4-dioxane. As presented in **Fig. 4a**, with the addition of SPC at  $r_{ox}$  1, 3, 5, and 8  
 269 the degradation of 1,4-dioxane was improved to 18.34, 22.11, 27.52 and 37.15% in 120 min, respectively.  
 270 The maximum degradation of 1,4-dioxane was attained at  $r_{ox}$  8, whereat the rate constant of 1,4-dioxane  
 271 degradation (**Table 3**) was increased from  $1.55 \times 10^{-3}$  to  $3.42 \times 10^{-3} \text{ min}^{-1}$  as compared to sole HC. With  
 272 an increase of SPC dosage to  $r_{ox}$  10, 31.94% of 1,4-dioxane was degraded in 120 and  $k$  was estimated as  
 273  $3.14 \times 10^{-3} \text{ min}^{-1}$ . These results suggest that the increase of SPC dosage above the optimal value led to the  
 274 quench of  $\text{HO}^\bullet$  radicals. Undesired  $\text{HO}^\bullet$  consumption of radicals can be caused by unreacted  $\text{H}_2\text{O}_2$ ,  
 275 saturated  $\text{O}_2$  and radical recombination reactions, which mainly lead to the formation of secondary radical  
 276 species with lower oxidation potential (**Eqs. 13-19**) [20,48]. In this study, the degradation efficiency of  
 277 1,4-dioxane in HC/SPC was highest at  $r_{ox}$  8 and the competition of scavenging reactions intensified at  $r_{ox}$   
 278 10. Such trend regarding to SPC activation has been addressed by previous studies [50,54]. According to  
 279 the obtained results,  $r_{ox}$  8 was selected as the optimal SPC dosage for further experiments.



287

288 **Figure 4.** Effect of SPC  $r_{ox}$  on the degradation 1,4-D in HC/SPC: (a) degradation efficiency, (b) pseudo-  
 289 first-order kinetic plots ( $[1,4-D]_0$  100 ppm,  $C_v$  0.27,  $pH_0$  5,  $20 \pm 2$  °C).

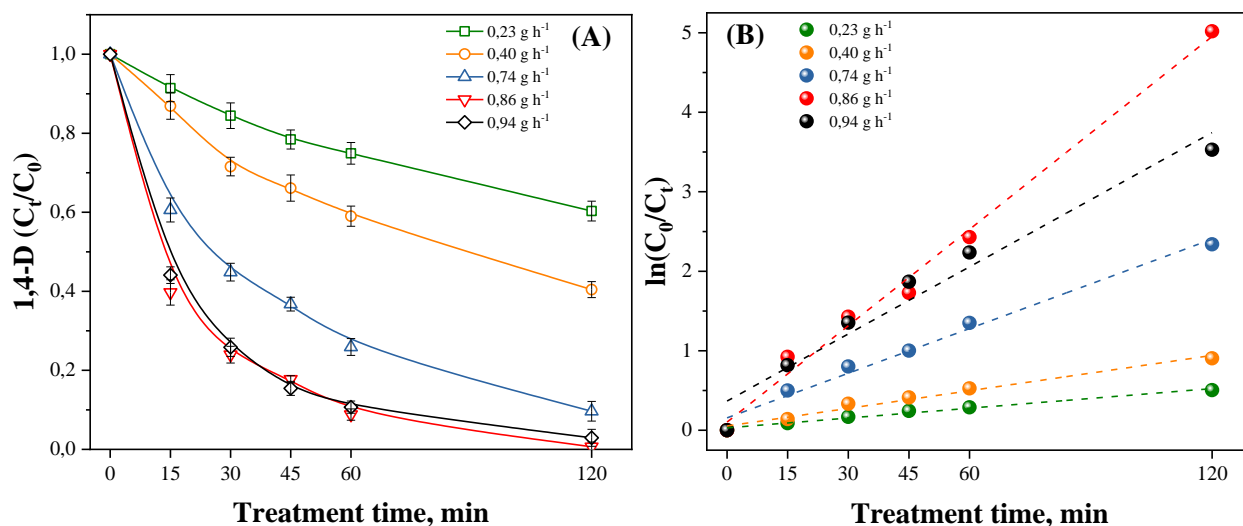
290 **Table 3.** Kinetic parameters of 1,4-dioxane degradation in HC/SPC at different  $r_{ox}$ .

	$r_{ox}$ 1	$r_{ox}$ 3	$r_{ox}$ 5	$r_{ox}$ 8	$r_{ox}$ 10
$k \times 10^{-2}, \text{min}^{-1}$	0.165	0.200	0.269	0.342	0.314
$R^2$	0.984	0.991	0.998	0.995	0.997

291

### 292 3.4 Effect of $O_3$ dosage

293 To investigate the effect of  $O_3$  dosage, the degradation of 1,4-dioxane was performed in HC/SPC at  $r_{ox}$  8  
 294 varying the dosage of  $O_3$  in the range of 0.23-0.94 g h<sup>-1</sup>. As can be seen from **Fig. 5a**, the increase of  $O_3$   
 295 dosage from 0.23 to 0.94 g h<sup>-1</sup> improved the degradation of 1,4-dioxane. Thus, 39.65, 59.55, 90.35 and  
 296 99.34% of 1,4-dioxane were degraded in HC/SPC with  $O_3$  dosage of 0.23, 0.40, 0.74 and 0.86 g h<sup>-1</sup> in 120  
 297 min, respectively. As given in **Table 4**, the increase of  $O_3$  dosage from 0.23 to 0.86 g h<sup>-1</sup> accelerated the  
 298 rate constant of 1,4-dioxane degradation from  $4.11 \times 10^{-3}$  to  $4.04 \times 10^{-2}$  min<sup>-1</sup>, respectively, while it was  
 299  $3.74 \times 10^{-3}$  min<sup>-1</sup> for HC/SPC at  $r_{ox}$  8 in absence of  $O_3$ . These finding suggest that the improvement effect  
 300 in HC/SPC/ $O_3$  was due to the reaction of  $O_3$  and  $H_2O_2$  yielding  $HO^\bullet$  radicals according to **Eqs. 8,9**  
 301 [55,56]. On the other hand, overpressure at Venturi tube inlet and the turbulence induced by HC provide  
 302 high transfer rate of  $O_3$  from gaseous phase into the liquid. In such scenario, the contact of  $O_3$  with  $H_2O_2$   
 303 is enhanced resulting in effective utilization of  $O_3$ . Particularly, the impact of HC is obvious when  
 304 comparing HC/SPC/ $O_3$  and SPC/ $O_3$  (**Fig. 2**), whereat 99.34 and 56.02% of 1,4-dioxane was degraded in  
 305 120 min and  $k$  values were  $4.04 \times 10^{-2}$  and  $6.60 \times 10^{-3}$  min<sup>-1</sup>, respectively. The outlet concentration of  $O_3$   
 306 during HC/SPC/ $O_3$  was determined as 0.135 g h<sup>-1</sup>, while it was 0.384 g h<sup>-1</sup> for SPC/ $O_3$ , confirming the  
 307 enhanced utilization efficiency of  $O_3$  due to the effect of HC.



308

309 **Figure 5.** Effect of O<sub>3</sub> dosage on the degradation 1,4-D in HC/SPC/O<sub>3</sub>: (a) degradation efficiency, (b)  
 310 pseudo-first-order kinetic plots ([1,4-D]<sub>0</sub> 100 ppm, C<sub>v</sub> 0.27, SPC *r*<sub>ox</sub> 8, pH<sub>0</sub> 5, 20±2 °C).

311 Although, an increase of inlet O<sub>3</sub> dosage increases the partial pressure of O<sub>3</sub> in gas phase and, thus,  
 312 improves the O<sub>3</sub> mass transfer [54], the increase of O<sub>3</sub> dosage to 0.94 g h<sup>-1</sup> decreased the degradation  
 313 efficiency to 97.12% resulting in the decrease of *k* from 4.04 × 10<sup>-2</sup> to 2.82 × 10<sup>-2</sup> min<sup>-1</sup>. Such effect can  
 314 be ascribed to the scavenging effect of high O<sub>3</sub> dosage, whereat a considerable amount of O<sub>3</sub> was  
 315 disintegrated to the consumption HO<sup>•</sup> radicals by dissolved O<sub>3</sub> as described in Eq. 20 [57]:

316



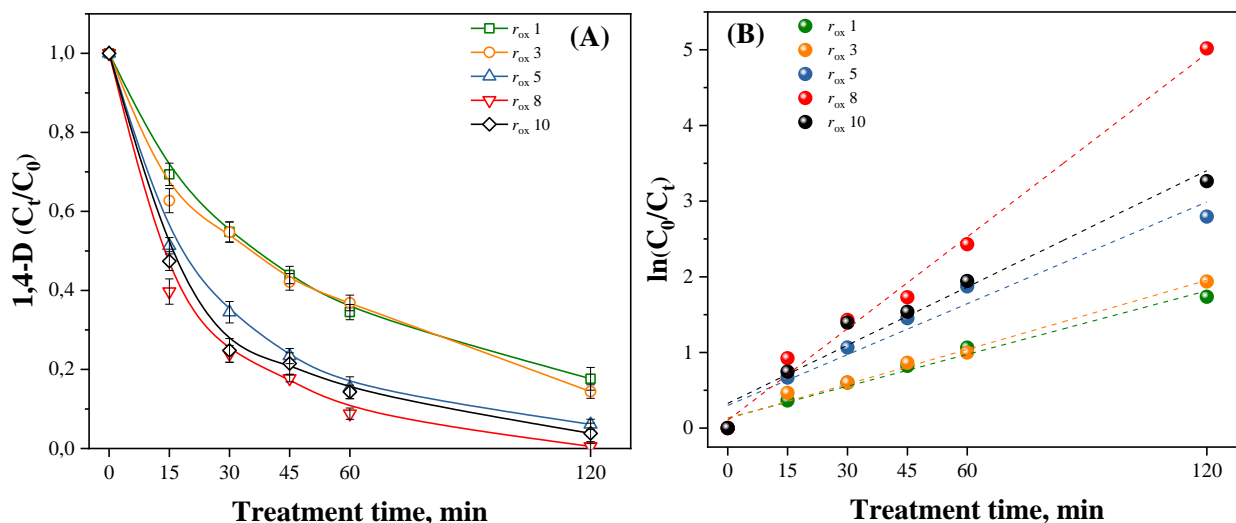
317 **Table 4.** Kinetic parameters of 1,4-dioxane degradation in HC/SPC/O<sub>3</sub> at *r*<sub>ox</sub> 8 and different O<sub>3</sub> dosage.

	O <sub>3</sub> dosage, g h <sup>-1</sup>				
	0.23	0.40	0.74	0.86	0.94
<i>k</i> × 10 <sup>-2</sup> , min <sup>-1</sup>	0.411	0.740	1.873	4.041	2.815
R <sup>2</sup>	0.984	0.980	0.986	0.992	0.961

318

319 To evaluate the improving effect of O<sub>3</sub> on HC/SPC, the degradation of 1,4-dioxane in HC/SPC/O<sub>3</sub> was  
 320 conducted with fixed dosage of O<sub>3</sub> at 0.86 g h<sup>-1</sup> and varying SPC *r*<sub>ox</sub> in the range of 1-10. As shown in  
 321 **Fig. 6a**, the degradation efficiency of 1,4-dioxane at *r*<sub>ox</sub> 1, 3, 5, 8 and 10 were improved from 18.34,  
 322 22.11, 27.52, 37.15% and 31.94% to 82.36, 85.58, 93.89, 99.34 and 96.18%, respectively. The  
 323 improvement effect of O<sub>3</sub> addition was the highest at *r*<sub>ox</sub> 8, which is clearly observed in **Table 5**. The  
 324 degradation rate of 1,4-dioxane was improved from 3.73 × 10<sup>-3</sup> to 4.04 × 10<sup>-2</sup> min<sup>-1</sup> at *r*<sub>ox</sub> 8, whereas the  
 325 corresponding *k* was increased from 3.20 × 10<sup>-3</sup> to 2.56 × 10<sup>-2</sup> min<sup>-1</sup> at *r*<sub>ox</sub> 10. These findings show that the

326 ratio between SPC and O<sub>3</sub> substantially defines the oxidative capacity of HC/SPC/O<sub>3</sub> towards 1,4-  
 327 dioxane.



328

329

330 **Figure 6.** Effect of fixed O<sub>3</sub> dosage on the degradation 1,4-D in HC/SPC/O<sub>3</sub> with various SPC  $r_{ox}$ : (a)  
 331 degradation efficiency, (b) pseudo-first-order kinetic plots ( $[1,4-D]_0$  100 ppm,  $C_v$  0.27,  $[O_3]$  0.86 g h<sup>-1</sup>,  
 332 pH<sub>0</sub> 5, 20±2 °C.

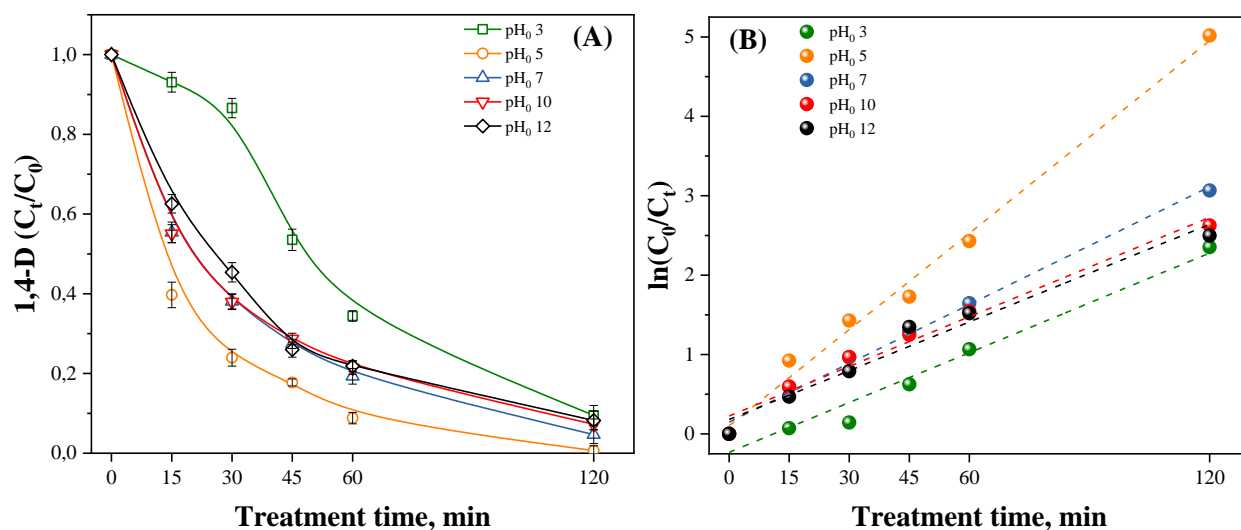
333 **Table 5.** Kinetic parameters of 1,4-dioxane degradation in HC/SPC/O<sub>3</sub> at 0.86 g h<sup>-1</sup> O<sub>3</sub> dosage and  
 334 different  $r_{ox}$ .

	$r_{ox}$ 1	$r_{ox}$ 3	$r_{ox}$ 5	$r_{ox}$ 8	$r_{ox}$ 10
$k \times 10^{-2}, \text{min}^{-1}$	1.401	1.524	2.242	4.041	2.563
$R^2$	0.979	0.984	0.956	0.992	0.963

335

### 336 3.5 Effect of initial pH

337 The solution pH is an important parameter, which significantly affect the production of reactive species  
 338 and, hence, the overall performance of HC/SPC/O<sub>3</sub> for the degradation of 1,4-dioxane. The effect of pH  
 339 also determines the oxidation potential of generated radical species, interaction between SPC and O<sub>3</sub> and  
 340 the state of the pollutant and oxidants in treated media. **Fig 7a** illustrates the effect of initial pH in the  
 341 range of 3-12 on the degradation of 1,4-dioxane in HC/SPC/O<sub>3</sub> process.



342

343

344 **Figure 7.** Effect of pH<sub>0</sub> on the degradation 1,4-D in HC/SPC/O<sub>3</sub>: (a) degradation efficiency, (b) pseudo-  
 345 first-order kinetic plots ([1,4-D]<sub>0</sub> 100 ppm, C<sub>v</sub> 0.27, SPC *r*<sub>ox</sub> 8, [O<sub>3</sub>] 0.86 g h<sup>-1</sup>, 20±2 °C).

346 According to **Fig. 7a**, the highest degradation efficiency was reached at pH<sub>0</sub> 5 (non-adjusted), while pH<sub>0</sub>  
 347 3, 7, 10 and 12 were detrimental. Among the tested pH values, the inhibitory effect of pH<sub>0</sub> 3 was the  
 348 highest resulting in 90.49% of 1,4-dioxane degradation within 120 min. This is attributed to the lower  
 349 decomposition rate of O<sub>3</sub> at acidic conditions, so the direct oxidation of 1,4-dioxane by molecular O<sub>3</sub> is  
 350 predominant at pH<sub>0</sub> 3. Since O<sub>3</sub> possess lower redox potential than HO<sup>•</sup> radicals, the direct oxidation  
 351 proceeded slowly resulting in the *k* value of  $2.09 \times 10^{-2} \text{ min}^{-1}$  (**Table 6**). In contrast, the rate constant of  
 352 1,4-dioxane degradation was markedly increased to  $4.04 \times 10^{-2} \text{ min}^{-1}$  at pH<sub>0</sub> 5, indicating high  
 353 concentration of generated radical species. This can be ascribed to the radical route of 1,4-dioxane  
 354 degradation *via* indirect O<sub>3</sub> oxidation and additional supply of HO<sup>•</sup> radicals due to the partial dissociation  
 355 of H<sub>2</sub>O<sub>2</sub>. The latter is initiated by the transformation of H<sub>2</sub>O<sub>2</sub> to yield HO<sub>2</sub><sup>-</sup> (**Eq. 11**), which further react  
 356 with O<sub>3</sub> as illustrated in **Eqs. 21-23** [58]. The detrimental effect of pH<sub>0</sub> < 5 coincides with the pH change  
 357 depicted in **Fig. 8**. Particularly, the degradation efficiency of 1,4-dioxane in HC/SPC/O<sub>3</sub> at pH<sub>0</sub> 3 was  
 358 markedly enhanced from 6.92 to 46.47% when the pH was increased from 3 to 6 after 45 min of  
 359 treatment.

360



361



362





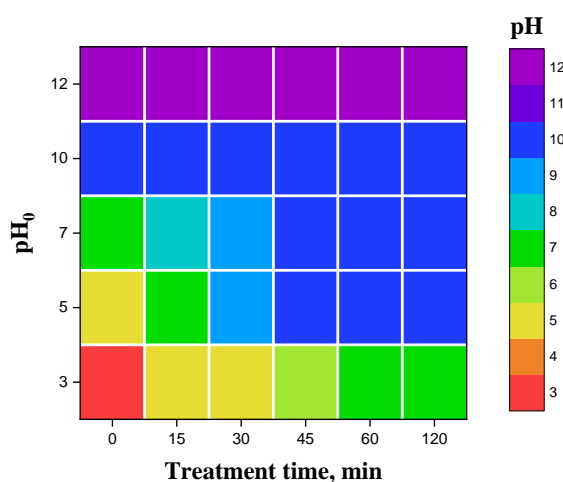
363

364 **Table 6.** Kinetic parameters of 1,4-dioxane degradation in HC/SPC/O<sub>3</sub> at different pH<sub>0</sub>.

	pH <sub>0</sub> 3	pH <sub>0</sub> 5	pH <sub>0</sub> 7	pH <sub>0</sub> 10	pH <sub>0</sub> 12
$k \times 10^{-2}, \text{min}^{-1}$	2.091	4.041	2.471	2.084	2.047
R <sup>2</sup>	0.968	0.992	0.993	0.977	0.968

365

366 Although alkaline pH promotes the decomposition of O<sub>3</sub>, the degradation efficiency of 1,4-dioxane in  
 367 HC/SPC/O<sub>3</sub> at pH<sub>0</sub> 10 and 12 was slightly decreased to 92.76 and 91.78%, respectively. Such trend can be  
 368 interpreted with an excessive production of HO<sub>2</sub><sup>-</sup> (Eq. 10), which act as a scavenger of HO<sup>•</sup> radicals (Eq.  
 369 24) [50,54,58].



370

371 **Figure 8.** The map of pH change throughout the degradation 1,4-D in HC/SPC/O<sub>3</sub> at various pH<sub>0</sub> ([1,4-  
 372 D]<sub>0</sub> 100 ppm, C<sub>v</sub> 0.27, SPC  $r_{ox}$  8, [O<sub>3</sub>] 0.86 g h<sup>-1</sup>, 20±2 °C).

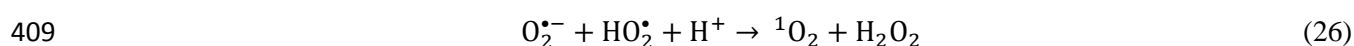
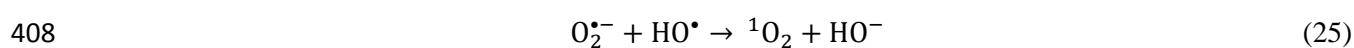
### 373 3.6 Identification of reactive species in HC/SPC/O<sub>3</sub>

374 Beside HO<sup>•</sup> radicals, O<sub>2</sub><sup>•-</sup> and CO<sub>3</sub><sup>•-</sup> radicals could be generated in HC/SPC/O<sub>3</sub> according to Eqs. 4-9, 17  
 375 and participate in the degradation of 1,4-dioxane. To evaluate the contribution of reactive species in  
 376 degradation of 1,4-dioxane, quenching experiments were conducted. Isopropyl alcohol (IPA), phenol  
 377 (PhOH), chloroform (CLF), *para*-benzoquinone (*p*-BQ) and sodium azide (NaN<sub>3</sub>) were utilized as  
 378 scavenging agents. The molar ratio of scavenger to SPC was set as 10:1 to ensure the effective quenching  
 379 of radicals. IPA rapidly reacts with HO<sup>•</sup> radicals ( $3.9 \times 10^9 \text{ M}^{-1} \text{ s}^{-1}$ ) and slowly responds to CO<sub>3</sub><sup>•-</sup> and O<sub>2</sub><sup>•-</sup>  
 380 radicals, with a rate constant of  $4.0 \times 10^4 \text{ M}^{-1} \text{ s}^{-1}$  and  $1.0 \times 10^6 \text{ M}^{-1} \text{ s}^{-1}$ , respectively [59,60]. Additionally,  
 381 the reaction of HO<sup>•</sup> radicals with IPA proceeds faster than with 1,4-dioxane ( $2.8 \times 10^9 \text{ M}^{-1} \text{ s}^{-1}$ ), H<sub>2</sub>O<sub>2</sub> ( $2.7$

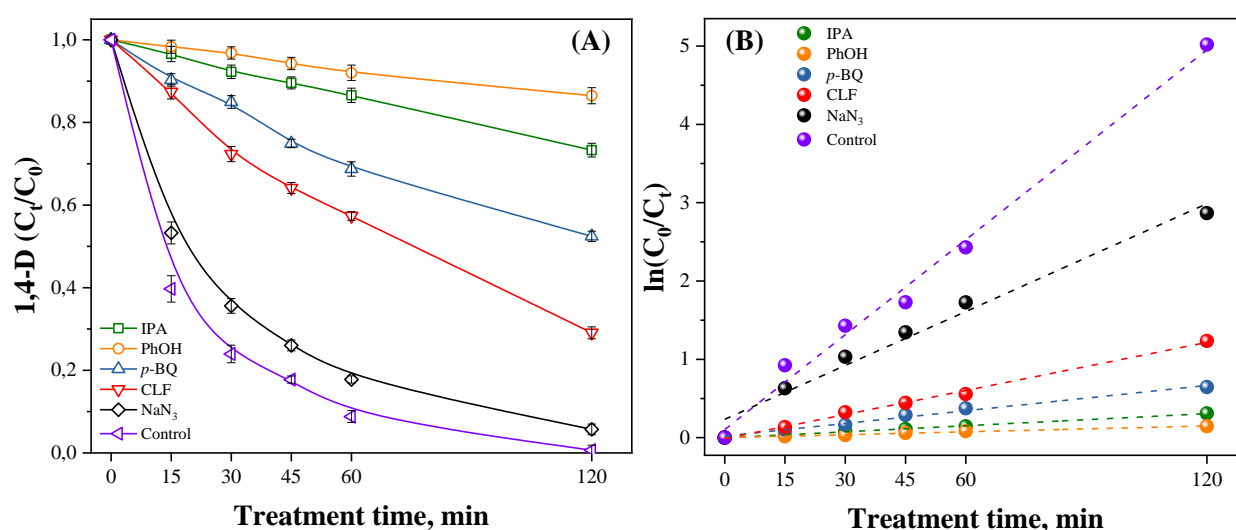


382  $\times 10^7 \text{ M}^{-1} \text{ s}^{-1}$ ),  $\text{HCO}_3^-$  ( $8.5 \times 10^6 \text{ M}^{-1} \text{ s}^{-1}$ ) and  $\text{CO}_3^{2-}$  ( $3.9 \times 10^8 \text{ M}^{-1} \text{ s}^{-1}$ ) [61–63], hence, IPA was selected to  
 383 study the existence of  $\text{HO}^\bullet$  radicals. On the other hand, PhOH was used to confirm the occurrence of  $\text{O}_2^{\bullet-}$   
 384 radicals as PhOH preferentially reacts with  $\text{HO}^\bullet$  ( $6 \times 10^8 \text{ M}^{-1} \text{ s}^{-1}$ ) and  $\text{CO}_3^{\bullet-}$  ( $1.2 \times 10^9 \text{ M}^{-1} \text{ s}^{-1}$ ) radicals  
 385 [60,64]. Additionally, the impact of  $\text{O}_2^{\bullet-}$  radicals was explored using *p*-BQ and CLF, which rapidly react  
 386 with a second-order rate constant of  $9.6 \times 10^8 \text{ M}^{-1} \text{ s}^{-1}$  and  $3.9 \times 10^{10} \text{ M}^{-1} \text{ s}^{-1}$ , respectively [39,59,65]. As  
 387 observed from **Fig. 9a**, the degradation efficiency of 1,4-dioxane was declined from 99.34 to 26.71%  
 388 after 120 min and the corresponding rate constants were decreased from  $4.04 \times 10^{-2}$  to  $2.58 \times 10^{-3} \text{ min}^{-1}$   
 389 (**Table 7**) in the presence of IPA. This illustrates the predominant role of  $\text{HO}^\bullet$  radicals. The degradation  
 390 efficiency of 1,4-dioxane was inhibited to 13.52% in 120 min with addition of PhOH, suggesting the  
 391 contribution of  $\text{O}_2^{\bullet-}$  radicals in 1,4-dioxane degradation. Based on these it can be proposed that for  
 392 HC/SPC/ $\text{O}_3$  highest contribution to degradation had  $\text{HO}^\bullet$  radicals, with moderate role of  $\text{CO}_3^{\bullet-}$  and minor  
 393 role of  $\text{O}_2^{\bullet-}$ . In contrast, the quenching experiments using *p*-BQ and CLF suppressed the degradation  
 394 efficiency of 1,4-dioxane by 52.99 and 29.21% in 120 min, respectively, suggesting a considerable  
 395 involvement of  $\text{O}_2^{\bullet-}$  radicals in degradation of 1,4-dioxane. It must be taken into account, that both  
 396 scavengers, but especially *p*-BQ also in some part can react with other radicals including  $\text{HO}^\bullet$ , thus these  
 397 tests are discussed as they confirmed contribution of superoxide radical in degradation. Additional aspect  
 398 that overlays on the performed tests relates to the fact, that although PhOH is low reactive towards  $\text{O}_2^{\bullet-}$   
 399 radicals ( $5.8 \times 10^2 \text{ M}^{-1} \text{ s}^{-1}$ ), scavenging of  $\text{HO}^\bullet$  radicals prohibits the regeneration of  $\text{O}_2^{\bullet-}$  radicals through  
 400 **Eq. 17**. In light of this “doubled” scavenging effect of PhOH it is confirmed that  $\text{O}_2^{\bullet-}$  contributed to the  
 401 degradation effect.

402 In the case of *p*-BQ and CLF, available (not scavenged so fast)  $\text{HO}^\bullet$  radicals promoted the continuous  
 403 regeneration of  $\text{O}_2^{\bullet-}$  radicals (**Eq. 17**). Interestingly, the inhibitory effect of hydrophobic and more volatile  
 404 CLF (which tends to move into the cavitation bubble - a place in the system that is less polar than water  
 405 and preferred by volatile compounds) was lower than *p*-BQ implying that the formation of  $\text{O}_2^{\bullet-}$  radicals  
 406 proceeds mainly in bulk liquid phase. Subsequent oxidation of  $\text{O}_2^{\bullet-}$  radicals by  $\text{HO}^\bullet$  and  $\text{HO}_2^\bullet$  radicals can  
 407 lead to the generation of singlet oxygen ( $^1\text{O}_2$ ) species through the following reactions [66]:



410 To elucidate the formation of  $^1\text{O}_2$  species,  $\text{NaN}_3$  was added to quench  $^1\text{O}_2$  with a rate constant of  $1 \times 10^9$   
 411  $\text{M}^{-1} \text{s}^{-1}$  [67]. Quenching experiments using  $\text{NaN}_3$  inhibited the degradation efficiency of 1,4-dioxane by  
 412 5.03%, whereat the corresponding degradation rate constant was decreased from  $4.04 \times 10^{-2}$  to  $2.29 \times 10^{-2}$   
 413  $\text{min}^{-1}$ . These observations suggest a negligible contribution of  $^1\text{O}_2$  in the degradation of 1,4-dioxane by  
 414 HC/SPC/ $\text{O}_3$ . Performed experiments provide general identification of ROSs. Besides above quenching  
 415 experiments, other techniques (e.g., electron paramagnetic resonance) can be suggested for the extensive  
 416 and more detailed analysis of ROSs in HC/SPC/ $\text{O}_3$ , as scavengers may interrupt radical chain reactions of  
 417  $\text{O}_3$  decomposition and consume  $\text{O}_3$  [68,69].



418  
 419 **Figure 9.** Effect of scavengers on the degradation 1,4-D in HC/SPC/ $\text{O}_3$ : (a) degradation efficiency, (b)  
 420 pseudo-first-order kinetic plots ( $[1,4\text{-D}]_0$  100 ppm,  $C_v$  0.27, SPC  $r_{\text{ox}}$  8,  $[\text{O}_3]$   $0.86 \text{ g h}^{-1}$ ,  $[\text{SPC}]:[\text{Scavenger}]$   
 421  $= 1:10$ ,  $20 \pm 2 \text{ }^\circ\text{C}$ ).

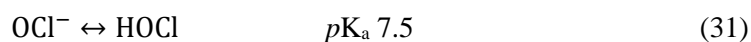
422 **Table 7.** Kinetic parameters of 1,4-dioxane degradation in HC/SPC/ $\text{O}_3$  in the presence of scavengers.

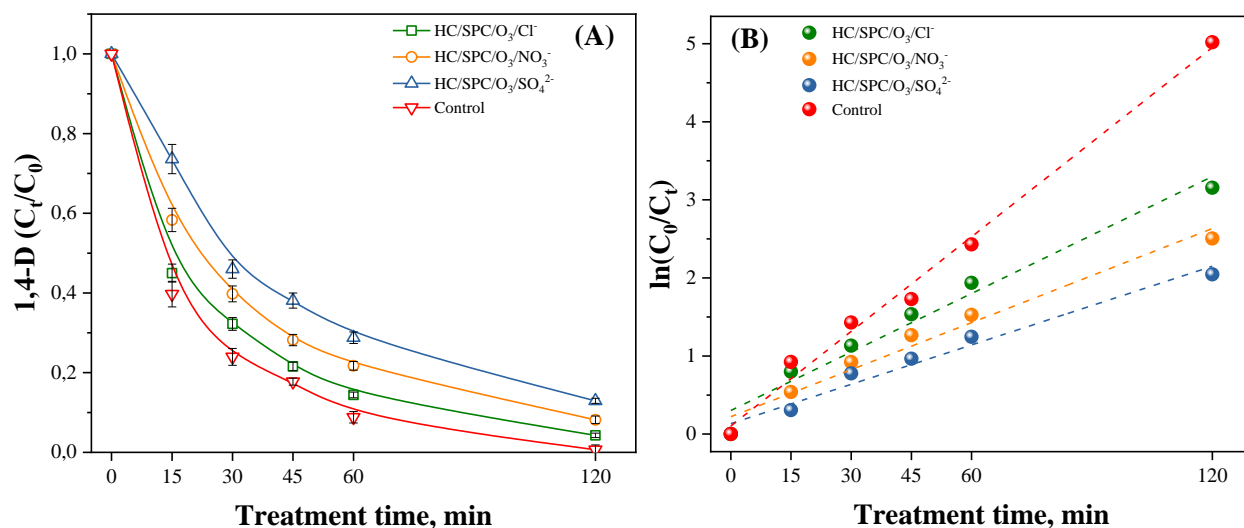
	Type of scavenger				
	IPA	PhOH	<i>p</i> -BQ	CLF	$\text{NaN}_3$
$k \times 10^{-2}, \text{min}^{-1}$	0.258	0.124	0.539	1.023	2.294
$R^2$	0.998	0.991	0.989	0.996	0.978

423  
 424 **3.7 The effect of co-existing inorganic anions on HC/SPC/ $\text{O}_3$**

425 Inorganic anions such as  $\text{Cl}^-$ ,  $\text{NO}_3^-$  and  $\text{SO}_4^{2-}$  are inherently present in natural water [70,71] and might  
 426 affect the performance of HC/SPC/ $\text{O}_3$ . Since the practical implementation of HC/SPC/ $\text{O}_3$  assumes the  
 427 treatment of contaminated natural water, the study of the effect of inorganic anions is required. To

428 evaluate the effect of inorganic anions, the degradation of 1,4-dioxane in HC/SPC/O<sub>3</sub> was conducted in  
 429 the presence of Cl<sup>-</sup>, NO<sub>3</sub><sup>-</sup> and SO<sub>4</sub><sup>2-</sup>, whereat the molar ratio of anion to SPC was 10:1. As shown, in **Fig.**  
 430 **10a**, the presence of Cl<sup>-</sup> anions resulted in a slight inhibitory effect decreasing the degradation efficiency  
 431 of 1,4-dioxane from 99.34 to 95.74% within 120 min. The inhibition effect of Cl<sup>-</sup> anions is commonly  
 432 ascribed to the formation chlorine species (i.e., Cl<sup>•</sup> and Cl<sub>2</sub><sup>•-</sup>) through the passage of reactions consuming  
 433 of HO<sup>•</sup> radicals as shown in **Eqs. 27-29**. However, the reaction of Cl<sup>-</sup> anions with HO<sup>•</sup> radicals is  
 434 negligible at circumneutral conditions due to the fast reverse reaction [72]. In this study, the inhibitory  
 435 effect of Cl<sup>-</sup> anions can be explained due to the interaction of Cl<sup>-</sup> anions with O<sub>3</sub>, which become relevant  
 436 at high Cl<sup>-</sup> concentration. Such interaction competes with H<sub>2</sub>O<sub>2</sub> for O<sub>3</sub> consumption and lead to the  
 437 formation of hypochlorite which exist in equilibrium with HClO (**Eqs. 30, 31**) and is not oxidized by O<sub>3</sub>  
 438 [72–74]. The inhibitory effect of 1,4-dioxane degradation in HC/SPC/O<sub>3</sub> found to be more deteriorate  
 439 with addition of NO<sub>3</sub><sup>-</sup> and SO<sub>4</sub><sup>2-</sup> anions. Thus, the presence of NO<sub>3</sub><sup>-</sup> and SO<sub>4</sub><sup>2-</sup> anions declined the  
 440 degradation efficiency of HC/SPC/O<sub>3</sub> towards 1,4-dioxane by 7.51 and 12.28% in 120 min, respectively.  
 441 Although, sulfate radicals (SO<sub>4</sub><sup>•-</sup>) formed *via* **Eq. 32** [75], exhibit relatively high oxidation potential and  
 442 selectivity towards electron-rich moieties, the presence of precursor SO<sub>4</sub><sup>2-</sup> anions showed the highest  
 443 inhibitory effect. This phenomenon can be referred to the decrease of the reduction potential of SO<sub>4</sub><sup>•-</sup>  
 444 radicals caused by the high concentration of SO<sub>4</sub><sup>2-</sup> anions [39]. As depicted in **Table 8**, the degradation  
 445 rate constant of 1,4-dioxane in presence of Cl<sup>-</sup>, NO<sub>3</sub><sup>-</sup> and SO<sub>4</sub><sup>2-</sup> anions in comparison with the process  
 446 without additives was decreased from 4.04 × 10<sup>-2</sup> to 2.50 × 10<sup>-2</sup>, 2.01 × 10<sup>-2</sup> and 1.68 × 10<sup>-2</sup> min<sup>-1</sup>,  
 447 respectively. In this study, the inhibitory effect of anions towards the degradation of 1,4-dioxane was in  
 448 the following order: SO<sub>4</sub><sup>2-</sup> > NO<sub>3</sub><sup>-</sup> > Cl<sup>-</sup>.





455

456

457

458

459

460

461

462

463

**Figure 10.** Effect of anions on the degradation 1,4-D in HC/SPC/O<sub>3</sub>: (a) degradation efficiency, (b)

pseudo-first-order kinetic plots ( $[1,4-D]_0$  100 ppm,  $C_v$  0.27, SPC  $r_{ox}$  8,  $[O_3]$  0.86 g h<sup>-1</sup>,  $[SPC]:[Anion] =$

1:10, 20±2 °C).

It is worth to mention, that in overall the inhibitory effect of anions was relatively low. In all cases above 80% degradation was obtained in 120 minutes. Applied concentration of anions was relatively high, thus in many real case scenarios it can be expected to be much lower. Thus, the developed system provides satisfactory performance to be implemented for treatment of real effluents.

**Table 8.** Kinetic parameters of 1,4-dioxane degradation in HC/SPC/O<sub>3</sub> in the presence of anions.

	Type of anion		
	Cl <sup>-</sup>	NO <sub>3</sub> <sup>-</sup>	SO <sub>4</sub> <sup>2-</sup>
$k \times 10^{-2}, \text{min}^{-1}$	2.497	2.009	1.681
R <sup>2</sup>	0.972	0.972	0.973

464

465

466

467

468

469

470

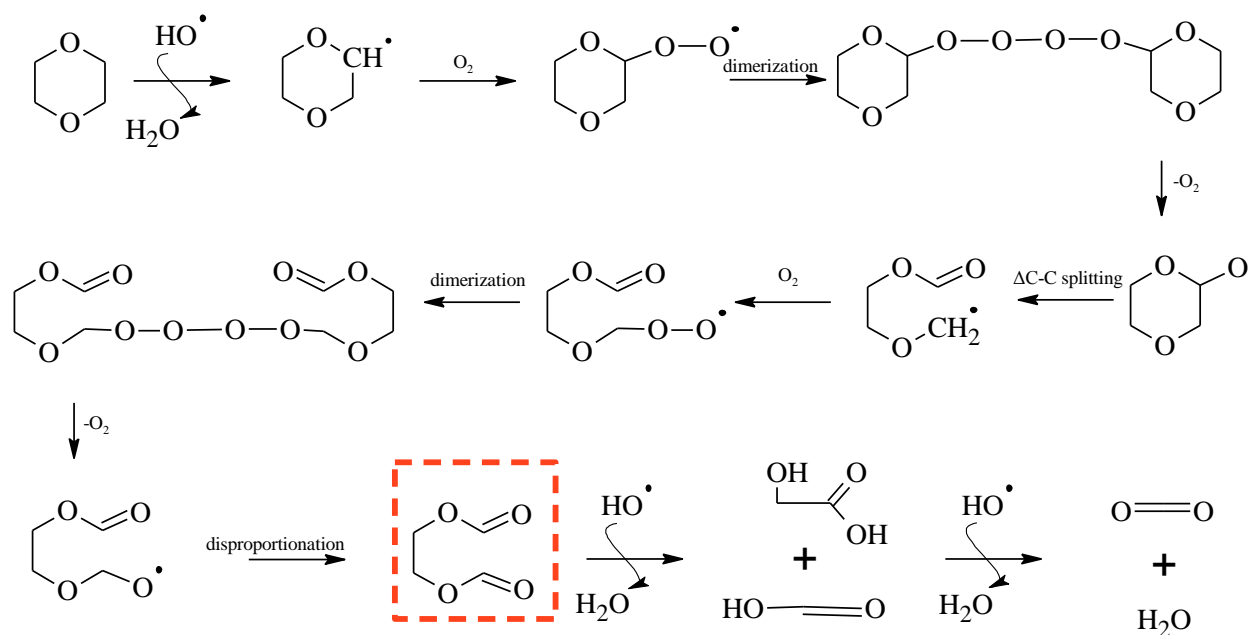
471

472

### 3.8 Degradation pathway of 1,4-dioxane in HC/SPC/O<sub>3</sub>

Highly reactive and non-selective behavior of radical species induces a broad variety of structural transformations to the target pollutant. These transformations can lead to the formation of by-products, which present toxicity higher than the parent compound. To better understand the transformation mechanism of 1,4-dioxane under HC/SPC/O<sub>3</sub>, the intermediates present in treated samples were identified and analyzed by GC-MS using SCAN mode. In order to detect minor intermediates and, thus propose an accurate pathway of 1,4-dioxane degradation in HC/SPC/O<sub>3</sub>, an initial concentration of 1000 ppm was adopted at fixed optimal  $r_{ox}$ . Based on the analysis of results, ethylene glycol diformate (EGDF) was

473 identified as the main intermediate of 1,4-dioxane degradation in HC/SPC/O<sub>3</sub> and the proposed  
 474 degradation pathway is presented in **Fig. 11**.



476 **Figure 11.** The proposed degradation pathway of 1,4-dioxane in HC/SPC/O<sub>3</sub>.

477

478 The initial step of the oxidative degradation of 1,4-dioxane proceeds through the attack of radical species  
 479 with H-abstraction to form 1,4-dioxanyl radical. In the presence of oxygen 1,4-dioxanyl radicals are  
 480 converted to peroxy radicals, which are further transformed into  $\alpha$ -oxyl radicals [9,76,77]. The latter is  
 481 recognized as a primary precursor of 1,4-dioxane degradation associated with AOPs. The presence of  
 482 EGDF in the treated samples supports the ring opening mechanism of  $\alpha$ -oxyl radical *via*  $\Delta$ C-C splitting at  
 483 the  $\alpha$ -C position [76,78]. The obtained radical reacts with oxygen and undergoes dimerization to form  
 484 tetraoxide, which is further fragmented to yield EGDF. Subsequent attack of HO $\cdot$  radicals causes  
 485 fragmentation of EGDF with formation of low-molecular intermediates (e.g., glycolic, formic acids),  
 486 which are further converted to CO<sub>2</sub> and H<sub>2</sub>O. TOC analysis of the samples showed up to 95% of TOC  
 487 removal confirming the mineralization of 1,4-dioxane (**Fig. S2**). Since, EDGF was found as the main by-  
 488 product of 1,4-dioxane degradation, the mechanism pathway of  $\Delta$ C-C splitting was predominant in  
 489 HC/SPC/O<sub>3</sub>. This result is consistent with the radical-type mechanism of 1,4-dioxane degradation  
 490 previously described for other AOPs.

491

492 3.9 *Economical evaluation*

493 Assessment of the economic feasibility of HC/SPC/O<sub>3</sub> was based on the energy efficiency and the  
494 treatment cost of 1,4-dioxane 100 ppm model solution, calculated for various studied processes compiled  
495 in **Table 9**. The cost of treatment was estimated using electric energy per order (E<sub>EO</sub>), which is defined as  
496 [79,80]:

$$497 \quad E_{EO} = \frac{P_{el} \times t \times 1000}{V \times 60 \times \log\left(\frac{C_0}{C_t}\right)} \quad (33)$$

498 , where P<sub>el</sub> is electric power (kW), t – time of treatment (min), V – volume of the treated solution (L), C<sub>0</sub>  
499 and C<sub>t</sub> are the initial and final concentration of the pollutant. Since log (C<sub>0</sub>/C<sub>t</sub>) = kt, the equation can be  
500 written as follows:

$$501 \quad E_{EO} = \frac{38.4 \times P_{el}}{V \times k} \quad (34)$$

502 The parameter E<sub>EO</sub> (kWh m<sup>-3</sup>order<sup>-1</sup>) describes the amount of energy required to degrade 90% of pollutant  
503 in 1 m<sup>3</sup> of the contaminated liquid. The calculations were conducted considering the power of HC system  
504 and O<sub>3</sub> generator, which were 0.16 and 0.38 kW, respectively. In this study, the E<sub>EO</sub> values of 1,4-dioxane  
505 degradation using HC/O<sub>3</sub> pH10, HC/H<sub>2</sub>O<sub>2</sub>/O<sub>3</sub>, HC/SPC/O<sub>3</sub> were 222.97, 165.89 and 102.65 kWh m<sup>-3</sup>  
506 order<sup>-1</sup>, respectively (**Table 9**). The adaptation of SPC in HC/SPC/O<sub>3</sub> decreased the energy consumption  
507 by 117 and 62% as compared to HC/O<sub>3</sub> pH10 and HC/H<sub>2</sub>O<sub>2</sub>/O<sub>3</sub>, respectively. This is attributed the higher  
508 degradation efficiency of HC/SPC/O<sub>3</sub>, which allowed to shorten the treatment time of 1,4-dioxane and,  
509 thereby decreased the energy consumption by HC pump and O<sub>3</sub> generator. Owing to cheaper industrial  
510 price, H<sub>2</sub>O<sub>2</sub> constituted only 0.8% of HC/H<sub>2</sub>O<sub>2</sub>/O<sub>3</sub> cost, while SPC accounted 6.4% of the total cost in  
511 HC/SPC/O<sub>3</sub>. However, the higher effectiveness of HC/SPC/O<sub>3</sub> provided a reduction of the total treatment  
512 cost by 52% as compared to HC/H<sub>2</sub>O<sub>2</sub>/O<sub>3</sub>.

513 In general, the ranges of E<sub>EO</sub> values determined for ozonation, peroxone and UV-based AOPs are 0.041-  
514 0.73, 0.86-5.96 and 0.73-499 kWh m<sup>-3</sup>, respectively, and can be substantially large depending on the  
515 pollutant's persistency [81]. Interestingly, the degradation of 1,4-dioxane using electro-peroxone and  
516 photo-electro-peroxone, according to data reported in the literature required 27.57 and 23.82 kWh m<sup>-3</sup>  
517 [10,11] (details of calculations are provided in **Supplementary data**). However, these values have only  
518 theoretical meaning as they were calculated using the theoretical energy required for O<sub>3</sub> generation and  
519 assuming the average cell voltage as 7.8 V [82,83]. It is well known that energetic effectiveness of ozone  
520 generators is far away from theoretical assumptions.



521 In this study,  $E_{EO}$  values were obtained based on nominal power of HC pump for used flowrate and real  
 522 power consumption of ozone generator. Therefore, the values of  $E_{EO}$  of HC-based AOPs for degradation  
 523 of 1,4-dioxane were generally higher as compared to reported in literature electro-peroxone and photo-  
 524 electro-peroxone. On the other hand, data presented in the cited papers do not allow to use typical formula  
 525 for  $E_{EO}$  that is commonly used and implemented in current paper. In addition, design of energy efficient  
 526 treatment systems will allow to reach more optimistic  $E_{EO}$  values reported in the literature.

527 **Table 9.** Evaluated cost of treatment of HC-based AOPs for degradation of 1,4-dioxane.

Process	$k, \text{min}^{-1}$	$E_{EO}, \text{kWh m}^{-3}\text{order}^{-1}$	Cost of energy*, USD	Amount of oxidant, kg	Cost of oxidant**, USD	Total cost, USD	Efficiency, %
HC/O <sub>3</sub> pH10	0.0186	222.97	24.53	-	-	24.53	89.89
HC/Peroxone	0.025	165.89	18.25	0.306	0.15	18.40	95.16
HC/SPC/O <sub>3</sub>	0.0404	102.65	11.29	1.413	0.78	12.07	99.34

528 \*The cost of energy was estimated based on the average electricity cost for industrial customers in Poland  
 529 - 0.11 USD/kWh.

530 \*\* The cost of industrial grade H<sub>2</sub>O<sub>2</sub> and SPC were assumed as 500, 550 USD/ton, respectively [84,85].

#### 531 4. Conclusions

532 HC/SPC/O<sub>3</sub> appears to be an effective alternative for the degradation of 1,4-dioxane resulting in 99.34%  
 533 in 120 min with a  $k$  of  $4.04 \times 10^{-2} \text{min}^{-1}$ . Compared to traditional peroxone process, HC/SPC/O<sub>3</sub> required  
 534 relatively lower dosages of SPC ( $r_{ox}$  8) and O<sub>3</sub> (0.86 g h<sup>-1</sup>), which is promising for practical  
 535 implementation in terms of economical feasibility. Concentrations of SPC and O<sub>3</sub> above/below the  
 536 optimal dosage were found detrimental due to the scavenging of radical species. The presence of CO<sub>3</sub><sup>2-</sup> in  
 537 HC/SPC/O<sub>3</sub> enabled the promotion of O<sub>3</sub> decomposition through the increase of pH and participated in  
 538 radical chain reactions to provide more reactive species. HO• radicals were determined as predominant  
 539 radical species in HC/SPC/O<sub>3</sub> according to the quenching experiments, which proposed the contribution  
 540 of reactive species in 1,4-dioxane degradation in order of HO• > CO<sub>3</sub><sup>•-</sup> > O<sub>2</sub><sup>•-</sup>. The studied co-existing  
 541 inorganic anions suppressed the effectiveness of HC/SPC/O<sub>3</sub>, whereat the inhibitory effect of SO<sub>4</sub><sup>2-</sup> anions  
 542 was higher than that of NO<sub>3</sub><sup>-</sup> and Cl<sup>-</sup> anions. The products of 1,4-dioxane degradation in HC/SPC/O<sub>3</sub> were  
 543 detected using GC-MS and the degradation pathway was proposed. The oxidation pathway included  
 544 several transformation steps with formation of ethylene glycol diformate, which is consistent with radical



545 route degradation 1,4-dioxane reported previously. This work highlights the potential application of SPC  
546 in peroxone process as an effective, safe and sustainable replacement to H<sub>2</sub>O<sub>2</sub> under HC.

547 **Acknowledgements**

548 The authors gratefully acknowledge financial support from the National Science Centre, Warsaw, Poland  
549 for project OPUS nr UMO-2017/25/B/ST8/01364

550 **References**

- 551 [1] M.J. Zenker, R.C. Borden, M.A. Barlaz, Occurrence and Treatment of 1,4-Dioxane in Aqueous  
552 Environments, *Environ. Eng. Sci.* 20 (2003) 423–432. doi:10.1089/109287503768335913.
- 553 [2] A. Abe, Distribution of 1,4-dioxane in relation to possible sources in the water environment, *Sci.*  
554 *Total Environ.* 227 (1999) 41–47. doi:10.1016/S0048-9697(99)00003-0.
- 555 [3] A. Yasuhara, Chemical components in leachates from hazardous wastes landfills in Japan,  
556 *Toxicol. Environ. Chem.* 51 (1995) 113–120. doi:10.1080/02772249509358229.
- 557 [4] C.A. Act, R. Act, R. Act, Environmental protection agency (EPA), Rep. Carcinog. 168 (2006).
- 558 [5] H. Barndök, L. Blanco, D. Hermosilla, Á. Blanco, Heterogeneous photo-Fenton processes using  
559 zero valent iron microspheres for the treatment of wastewaters contaminated with 1,4-dioxane,  
560 *Chem. Eng. J.* 284 (2016) 112–121. doi:10.1016/J.CEJ.2015.08.097.
- 561 [6] C.D. Adams, P.A. Scanlan, N.D. Secrist, Oxidation and biodegradability enhancement of 1, 4-  
562 dioxane using hydrogen peroxide and ozone, *Environ. Sci. Technol.* 28 (1994) 1812–1818.
- 563 [7] H. Barndök, D. Hermosilla, C. Negro, Á. Blanco, Comparison and Predesign Cost Assessment of  
564 Different Advanced Oxidation Processes for the Treatment of 1,4-Dioxane-Containing  
565 Wastewater from the Chemical Industry, *ACS Sustain. Chem. Eng.* 6 (2018) 5888–5894.  
566 doi:10.1021/acssuschemeng.7b04234.
- 567 [8] M.P. Rayaroth, D. Oh, C.S. Lee, Y.G. Kang, Y.S. Chang, In situ chemical oxidation of  
568 contaminated groundwater using a sulfidized nanoscale zerovalent iron–persulfate system:  
569 Insights from a box-type study, *Chemosphere.* 257 (2020) 127117.  
570 doi:10.1016/j.chemosphere.2020.127117.
- 571 [9] S. Sonawane, K. Fedorov, M.P. Rayaroth, G. Boczkaj, Degradation of 1,4-dioxane by sono-  
572 activated persulfates for water and wastewater treatment applications, *Water Resour. Ind.* 28  
573 (2022) 100183. doi:10.1016/J.WRI.2022.100183.
- 574 [10] W. Shen, Y. Wang, J. Zhan, B. Wang, J. Huang, S. Deng, G. Yu, Kinetics and operational



- 575 parameters for 1,4-dioxane degradation by the photoelectro-peroxone process, *Chem. Eng. J.* 310  
576 (2017) 249–258. doi:10.1016/J.CEJ.2016.10.111.
- 577 [11] H. Wang, B. Bakheet, S. Yuan, X. Li, G. Yu, S. Murayama, Y. Wang, Kinetics and energy  
578 efficiency for the degradation of 1,4-dioxane by electro-peroxone process, *J. Hazard. Mater.* 294  
579 (2015) 90–98. doi:10.1016/j.jhazmat.2015.03.058.
- 580 [12] M.P. Rayaroth, C.T. Aravindakumar, N.S. Shah, G. Boczkaj, Advanced oxidation processes  
581 (AOPs) based wastewater treatment - unexpected nitration side reactions - a serious environmental  
582 issue: A review, *Chem. Eng. J.* 430 (2022) 133002. doi:10.1016/J.CEJ.2021.133002.
- 583 [13] N. Takahashi, T. Hibino, H. Torii, S. Shibata, S. Tasaka, J. Yoneya, M. Matsuda, H. Ogasawara,  
584 K. Sugimoto, T. Fujioka, Evaluation of O<sub>3</sub>/UV and O<sub>3</sub>/H<sub>2</sub>O<sub>2</sub> as Practical Advanced Oxidation  
585 Processes for Degradation of 1,4-Dioxane, *Ozone Sci. Eng.* 35 (2013) 331–337.  
586 doi:10.1080/01919512.2013.795851.
- 587 [14] M. Abdi, M. Balagabri, H. Karimi, H. Hossini, S.O. Rastegar, Degradation of crystal violet (CV)  
588 from aqueous solutions using ozone, peroxone, electroperoxone, and electrolysis processes: a  
589 comparison study, *Appl. Water Sci.* 10 (2020) 168. doi:10.1007/s13201-020-01252-w.
- 590 [15] H. Chen, J. Wang, Degradation and mineralization of ofloxacin by ozonation and peroxone  
591 (O<sub>3</sub>/H<sub>2</sub>O<sub>2</sub>) process, *Chemosphere.* 269 (2020) 128775. doi:10.1016/j.chemosphere.2020.128775.
- 592 [16] I. Epold, N. Dulova, Y. Veressinina, M. Trapido, Application of Ozonation, UV Photolysis,  
593 Fenton Treatment and other Related Processes for Degradation of Ibuprofen and  
594 Sulfamethoxazole in Different Aqueous Matrices, *J. Adv. Oxid. Technol.* 15 (2012) 354–364.  
595 doi:doi:10.1515/jaots-2012-0215.
- 596 [17] M. Gagol, A. Przyjazny, G. Boczkaj, Highly effective degradation of selected groups of organic  
597 compounds by cavitation based AOPs under basic pH conditions, *Ultrason. Sonochem.* 45 (2018)  
598 257–266. doi:10.1016/j.ultsonch.2018.03.013.
- 599 [18] G. Boczkaj, A. Fernandes, P. Makoś, Study of Different Advanced Oxidation Processes for  
600 Wastewater Treatment from Petroleum Bitumen Production at Basic pH, *Ind. Eng. Chem. Res.*  
601 (2017). doi:10.1021/acs.iecr.7b01507.
- 602 [19] G. Boczkaj, A. Fernandes, Wastewater treatment by means of advanced oxidation processes at  
603 basic pH conditions: A review, *Chem. Eng. J.* 320 (2017) 608–633.

- 604 doi:10.1016/J.CEJ.2017.03.084.
- 605 [20] X. Liu, S. He, Y. Yang, B. Yao, Y. Tang, L. Luo, D. Zhi, Z. Wan, L. Wang, Y. Zhou, A review on  
606 percarbonate-based advanced oxidation processes for remediation of organic compounds in water,  
607 Environ. Res. 200 (2021) 111371. doi:10.1016/J.ENVRES.2021.111371.
- 608 [21] A. Eslami, F. Mehdipour, K.Y.A. Lin, H. Sharifi Maleksari, F. Mirzaei, F. Ghanbari, Sono-photo  
609 activation of percarbonate for the degradation of organic dye: The effect of water matrix and  
610 identification of by-products, J. Water Process Eng. 33 (2020) 100998.  
611 doi:10.1016/J.JWPE.2019.100998.
- 612 [22] X. Ling, J. Deng, C. Ye, A. Cai, S. Ruan, M. Chen, X. Li, Fe(II)-activated sodium percarbonate  
613 for improving sludge dewaterability: Experimental and theoretical investigation combined with the  
614 evaluation of subsequent utilization, Sci. Total Environ. 799 (2021) 149382.  
615 doi:10.1016/J.SCITOTENV.2021.149382.
- 616 [23] Z. Miao, X. Gu, S. Lu, X. Zang, X. Wu, M. Xu, L.B.B. Ndong, Z. Qiu, Q. Sui, G.Y. Fu,  
617 Perchloroethylene (PCE) oxidation by percarbonate in Fe<sup>2+</sup>-catalyzed aqueous solution: PCE  
618 performance and its removal mechanism, Chemosphere. 119 (2015) 1120–1125.  
619 doi:10.1016/J.CHEMOSPHERE.2014.09.065.
- 620 [24] X. Zang, X. Gu, S. Lu, Z. Miao, X. Zhang, X. Fu, G.Y. Fu, Z. Qiu, Q. Sui, Enhanced degradation  
621 of trichloroethene by sodium percarbonate activated with Fe(II) in the presence of citric acid,  
622 Water Supply. 17 (2016) 665–673. doi:10.2166/ws.2016.117.
- 623 [25] U. Farooq, M. Danish, S. Lu, M.L. Brusseau, M. Naqvi, X. Fu, X. Zhang, Q. Sui, Z. Qiu, Efficient  
624 transformation in characteristics of cations supported-reduced graphene oxide nanocomposites for  
625 the destruction of trichloroethane, Appl. Catal. A Gen. 544 (2017) 10–20.  
626 doi:10.1016/J.APCATA.2017.07.007.
- 627 [26] D. Li, Y. Xiao, M. Pu, J. Zan, S. Zuo, H. Xu, D. Xia, A metal-free protonated g-C<sub>3</sub>N<sub>4</sub> as an  
628 effective sodium percarbonate activator at ambient pH conditions: Efficiency, stability and  
629 mechanism, Mater. Chem. Phys. 231 (2019) 225–232.  
630 doi:10.1016/J.MATCHEMPHYS.2019.04.016.
- 631 [27] M. Danish, X. Gu, S. Lu, U. Farooq, W.Q. Zaman, X. Fu, Z. Miao, M.L. Brusseau, A. Ahmad, M.  
632 Naqvi, An efficient catalytic degradation of trichloroethene in a percarbonate system catalyzed by

- 633 ultra-fine heterogeneous zeolite supported zero valent iron-nickel bimetallic composite, *Appl.*  
634 *Catal. A Gen.* 531 (2017) 177–186. doi:10.1016/J.APCATA.2016.11.001.
- 635 [28] L. Li, J. Huang, X. Hu, S. Zhang, Q. Dai, H. Chai, L. Gu, Activation of sodium percarbonate by  
636 vanadium for the degradation of aniline in water: Mechanism and identification of reactive  
637 species, *Chemosphere.* 215 (2019) 647–656. doi:10.1016/J.CHEMOSPHERE.2018.10.047.
- 638 [29] J. Rivas, O. Gimeno, T. Borralho, F. Beltrán, Influence of oxygen and free radicals promoters on  
639 the UV-254 nm photolysis of diclofenac, *Chem. Eng. J.* 163 (2010) 35–40.  
640 doi:10.1016/J.CEJ.2010.07.027.
- 641 [30] V. Shafirovich, A. Dourandin, W. Huang, N.E. Geacintov, The Carbonate Radical Is a Site-  
642 selective Oxidizing Agent of Guanine in Double-stranded Oligonucleotides \*, *J. Biol. Chem.* 276  
643 (2001) 24621–24626. doi:10.1074/jbc.M101131200.
- 644 [31] J.S. Moore, G.O. Phillips, A. Sosnowski, Reaction of carbonate radical anion with substituted  
645 phenols, *Int. J. Radiat. Biol.* 31 (1977) 605.
- 646 [32] J.P. Huang, S.A. Mabury, A new method for measuring carbonate radical reactivity toward  
647 pesticides, *Environ. Toxicol. Chem.* 19 (2000) 1507.
- 648 [33] M.P. Rayaroth, U.K. Aravind, C.T. Aravindakumar, Effect of inorganic ions on the ultrasound  
649 initiated degradation and product formation of triphenylmethane dyes, *Ultrason. Sonochem.* 48  
650 (2018) 482–491. doi:10.1016/j.ultsonch.2018.07.009.
- 651 [34] S. Canonica, T. Kohn, M. Mac, F.J. Real, J. Wirz, U. von Gunten, Photosensitizer Method to  
652 Determine Rate Constants for the Reaction of Carbonate Radical with Organic Compounds,  
653 *Environ. Sci. Technol.* 39 (2005) 9182–9188. doi:10.1021/es051236b.
- 654 [35] B.C. Hodges, E.L. Cates, J.-H. Kim, Challenges and prospects of advanced oxidation water  
655 treatment processes using catalytic nanomaterials, *Nat. Nanotechnol.* 13 (2018) 642–650.  
656 doi:10.1038/s41565-018-0216-x.
- 657 [36] K. Fedorov, K. Dinesh, X. Sun, R. Darvishi Cheshmeh Soltani, Z. Wang, S. Sonawane, G.  
658 Boczkaj, Synergistic effects of hybrid advanced oxidation processes (AOPs) based on  
659 hydrodynamic cavitation phenomenon – A review, *Chem. Eng. J.* 432 (2022) 134191.  
660 doi:10.1016/J.CEJ.2021.134191.
- 661 [37] E. Cako, R. Darvishi Cheshmeh Soltani, X. Sun, G. Boczkaj, Desulfurization of raw naphtha cuts

- 662 using hybrid systems based on acoustic cavitation and advanced oxidation processes (AOPs),  
663 Chem. Eng. J. 439 (2022) 135354. doi:10.1016/J.CEJ.2022.135354.
- 664 [38] A.J. Barik, P.R. Gogate, Hybrid treatment strategies for 2,4,6-trichlorophenol degradation based  
665 on combination of hydrodynamic cavitation and AOPs, Ultrason. Sonochem. 40 (2018) 383–394.  
666 doi:10.1016/j.ultsonch.2017.07.029.
- 667 [39] K. Fedorov, X. Sun, G. Boczkaj, Combination of hydrodynamic cavitation and SR-AOPs for  
668 simultaneous degradation of BTEX in water, Chem. Eng. J. (2020).  
669 doi:10.1016/j.cej.2020.128081.
- 670 [40] P.R. Gogate, G.S. Bhosale, Comparison of effectiveness of acoustic and hydrodynamic cavitation  
671 in combined treatment schemes for degradation of dye wastewaters, Chem. Eng. Process. Process  
672 Intensif. 71 (2013) 59–69. doi:10.1016/j.cep.2013.03.001.
- 673 [41] M. Gągól, A. Przyjazny, G. Boczkaj, Effective method of treatment of industrial effluents under  
674 basic pH conditions using acoustic cavitation – A comprehensive comparison with hydrodynamic  
675 cavitation processes, Chem. Eng. Process. - Process Intensif. 128 (2018) 103–113.  
676 doi:10.1016/J.CEP.2018.04.010.
- 677 [42] M. Dular, T. Griessler-Bulc, I. Gutierrez-Aguirre, E. Heath, T. Kosjek, A. Krivograd Klemenčič,  
678 M. Oder, M. Petkovšek, N. Rački, M. Ravnikar, A. Šarc, B. Širok, M. Zupanc, M. Žitnik, B.  
679 Kompare, Use of hydrodynamic cavitation in (waste)water treatment, Ultrason. Sonochem. 29  
680 (2016) 577–588. doi:10.1016/J.ULTSONCH.2015.10.010.
- 681 [43] P. Makoś, A. Fernandes, G. Boczkaj, Method for the simultaneous determination of monoaromatic  
682 and polycyclic aromatic hydrocarbons in industrial effluents using dispersive liquid–liquid  
683 microextraction with gas chromatography–mass spectrometry, J. Sep. Sci. 41 (2018) 2360–2367.  
684 doi:10.1002/jssc.201701464.
- 685 [44] B. Wang, H. Su, B. Zhang, Hydrodynamic cavitation as a promising route for wastewater  
686 treatment – A review, Chem. Eng. J. 412 (2021) 128685. doi:10.1016/J.CEJ.2021.128685.
- 687 [45] M. Gągól, A. Przyjazny, G. Boczkaj, Wastewater treatment by means of advanced oxidation  
688 processes based on cavitation – A review, Chem. Eng. J. 338 (2018) 599–627.  
689 doi:10.1016/J.CEJ.2018.01.049.
- 690 [46] P.R. Gogate, A.B. Pandit, HYDRODYNAMIC CAVITATION REACTORS: A STATE OF THE

- 691 ART REVIEW, *Rev. Chem. Eng.* 17 (2001) 1–85. doi:10.1515/revce.2001.17.1.1.
- 692 [47] A. Mukherjee, A. Mullick, P. Vadthya, S. Moulik, A. Roy, Surfactant degradation using  
693 hydrodynamic cavitation based hybrid advanced oxidation technology: A techno economic  
694 feasibility study, *Chem. Eng. J.* 398 (2020) 125599. doi:10.1016/J.CEJ.2020.125599.
- 695 [48] G. Boczkaj, M. Gągol, M. Klein, A. Przyjazny, Effective method of treatment of effluents from  
696 production of bitumens under basic pH conditions using hydrodynamic cavitation aided by  
697 external oxidants, *Ultrason. Sonochem.* 40 (2018) 969–979.  
698 doi:10.1016/J.ULTSONCH.2017.08.032.
- 699 [49] J.A.I. Pimentel, C. Di Dong, S. Garcia-Segura, R.R.M. Abarca, C.W. Chen, M.D.G. de Luna,  
700 Degradation of tetracycline antibiotics by Fe<sup>2+</sup>-catalyzed percarbonate oxidation, *Sci. Total*  
701 *Environ.* 781 (2021) 146411. doi:10.1016/J.SCITOTENV.2021.146411.
- 702 [50] C. Tan, Q. Xu, H. Zhang, Z. Liu, S. Ren, H. Li, Enhanced removal of coumarin by a novel  
703 O<sub>3</sub>/SPC system: Kinetic and mechanism, *Chemosphere.* 219 (2019) 100–108.  
704 doi:10.1016/J.CHEMOSPHERE.2018.11.194.
- 705 [51] S.D. Patton, M.C. Dodd, H. Liu, Degradation of 1,4-dioxane by reactive species generated during  
706 breakpoint chlorination: Proposed mechanisms and implications for water treatment and reuse, *J.*  
707 *Hazard. Mater. Lett.* 3 (2022) 100054. doi:https://doi.org/10.1016/j.hazl.2022.100054.
- 708 [52] P. Neta, R.E. Huie, A.B. Ross, Rate Constants for Reactions of Inorganic Radicals in Aqueous  
709 Solution, *J. Phys. Chem. Ref. Data.* 17 (1988) 1027–1284. doi:10.1063/1.555808.
- 710 [53] V. Maurino, P. Calza, C. Minero, E. Pelizzetti, M. Vincenti, Light-assisted 1,4-dioxane  
711 degradation, *Chemosphere.* 35 (1997) 2675–2688. doi:https://doi.org/10.1016/S0045-  
712 6535(97)00322-6.
- 713 [54] X. Yu, M. Kamali, P. Van Aken, L. Appels, B. Van der Bruggen, R. Dewil, Synergistic effects of  
714 the combined use of ozone and sodium percarbonate for the oxidative degradation of dichlorvos, *J.*  
715 *Water Process Eng.* 39 (2021) 101721. doi:10.1016/J.JWPE.2020.101721.
- 716 [55] M. Gągol, A. Przyjazny, G. Boczkaj, Wastewater treatment by means of advanced oxidation  
717 processes based on cavitation – A review, *Chem. Eng. J.* 338 (2018) 599–627.  
718 doi:10.1016/j.cej.2018.01.049.
- 719 [56] G. Merényi, J. Lind, S. Naumov, C. von Sonntag, Reaction of Ozone with Hydrogen Peroxide

- 720 (Peroxo Process): A Revision of Current Mechanistic Concepts Based on Thermokinetic and  
721 Quantum-Chemical Considerations, *Environ. Sci. Technol.* 44 (2010) 3505–3507.  
722 doi:10.1021/es100277d.
- 723 [57] S. Tang, D. Yuan, Y. Rao, M. Li, G. Shi, J. Gu, T. Zhang, Percarbonate promoted antibiotic  
724 decomposition in dielectric barrier discharge plasma, *J. Hazard. Mater.* 366 (2019) 669–676.  
725 doi:10.1016/J.JHAZMAT.2018.12.056.
- 726 [58] H. Guo, D. Li, Z. Li, S. Lin, Y. Wang, S. Pan, J. Han, Promoted elimination of antibiotic  
727 sulfamethoxazole in water using sodium percarbonate activated by ozone: Mechanism,  
728 degradation pathway and toxicity assessment, *Sep. Purif. Technol.* 266 (2021) 118543.  
729 doi:10.1016/J.SEPPUR.2021.118543.
- 730 [59] P. Yan, Q. Sui, S. Lyu, H. Hao, H.F. Schröder, W. Gebhardt, Elucidation of the oxidation  
731 mechanisms and pathways of sulfamethoxazole degradation under Fe(II) activated percarbonate  
732 treatment, *Sci. Total Environ.* 640–641 (2018) 973–980. doi:10.1016/J.SCITOTENV.2018.05.315.
- 733 [60] Y. Xiao, X. Liu, Y. Huang, W. Kang, Z. Wang, H. Zheng, Roles of hydroxyl and carbonate  
734 radicals in bisphenol a degradation via a nanoscale zero-valent iron/percarbonate system:  
735 influencing factors and mechanisms, *RSC Adv.* 11 (2021) 3636–3644. doi:10.1039/D0RA08395J.
- 736 [61] M. Bagheri, M. Mohseni, Pilot-scale treatment of 1,4-dioxane contaminated waters using 185 nm  
737 radiation: Experimental and CFD modeling, *J. Water Process Eng.* 19 (2017) 185–192.  
738 doi:https://doi.org/10.1016/j.jwpe.2017.06.015.
- 739 [62] G. Imoberdorf, M. Mohseni, Kinetic study and modeling of the vacuum-UV photoinduced  
740 degradation of 2,4-D, *Chem. Eng. J.* 187 (2012) 114–122.  
741 doi:https://doi.org/10.1016/j.cej.2012.01.107.
- 742 [63] J.C. Crittenden, S. Hu, D.W. Hand, S.A. Green, A kinetic model for H<sub>2</sub>O<sub>2</sub>/UV process in a  
743 completely mixed batch reactor, *Water Res.* 33 (1999) 2315–2328.  
744 doi:https://doi.org/10.1016/S0043-1354(98)00448-5.
- 745 [64] J. Gao, X. Duan, K. O'Shea, D.D. Dionysiou, Degradation and transformation of bisphenol A in  
746 UV/Sodium percarbonate: Dual role of carbonate radical anion, *Water Res.* 171 (2020) 115394.  
747 doi:10.1016/J.WATRES.2019.115394.
- 748 [65] A.L. Teel, R.J. Watts, Degradation of carbon tetrachloride by modified Fenton's reagent, J.



- 749 Hazard. Mater. 94 (2002) 179–189. doi:10.1016/S0304-3894(02)00068-7.
- 750 [66] Y. Nosaka, A.Y. Nosaka, Generation and Detection of Reactive Oxygen Species in Photocatalysis,  
751 Chem. Rev. 117 (2017) 11302–11336. doi:10.1021/acs.chemrev.7b00161.
- 752 [67] S. Zhu, X. Li, J. Kang, X. Duan, S. Wang, Persulfate Activation on Crystallographic Manganese  
753 Oxides: Mechanism of Singlet Oxygen Evolution for Nonradical Selective Degradation of  
754 Aqueous Contaminants, Environ. Sci. Technol. 53 (2019) 307–315. doi:10.1021/acs.est.8b04669.
- 755 [68] Y. Guo, J. Long, J. Huang, G. Yu, Y. Wang, Can the commonly used quenching method really  
756 evaluate the role of reactive oxygen species in pollutant abatement during catalytic ozonation?,  
757 Water Res. 215 (2022) 118275. doi:https://doi.org/10.1016/j.watres.2022.118275.
- 758 [69] Y. Wang, G. Yu, Challenges and pitfalls in the investigation of the catalytic ozonation mechanism:  
759 A critical review, J. Hazard. Mater. 436 (2022) 129157.  
760 doi:https://doi.org/10.1016/j.jhazmat.2022.129157.
- 761 [70] J. Wang, S. Wang, Effect of inorganic anions on the performance of advanced oxidation processes  
762 for degradation of organic contaminants, Chem. Eng. J. 411 (2021) 128392.  
763 doi:10.1016/J.CEJ.2020.128392.
- 764 [71] M.P. Rayaroth, U.K. Aravind, C.T. Aravindakumar, Effect of inorganic ions on the ultrasound  
765 initiated degradation and product formation of triphenylmethane dyes, Ultrason. Sonochem. 48  
766 (2018) 482–491. doi:10.1016/J.ULTSONCH.2018.07.009.
- 767 [72] U. von Gunten, Ozonation of drinking water: Part II. Disinfection and by-product formation in  
768 presence of bromide, iodide or chlorine, Water Res. 37 (2003) 1469–1487.  
769 doi:https://doi.org/10.1016/S0043-1354(02)00458-X.
- 770 [73] W.R. Haag, J. Hoigné, Ozonation of water containing chlorine or chloramines. Reaction products  
771 and kinetics, Water Res. 17 (1983) 1397–1402. doi:https://doi.org/10.1016/0043-1354(83)90270-  
772 1.
- 773 [74] A. Asghar, H. V Lutze, J. Tuerk, T.C. Schmidt, Influence of water matrix on the degradation of  
774 organic micropollutants by ozone based processes: A review on oxidant scavenging mechanism, J.  
775 Hazard. Mater. 429 (2022) 128189. doi:https://doi.org/10.1016/j.jhazmat.2021.128189.
- 776 [75] M. Khajeh, M.M. Amin, A. Fatehizadeh, T.M. Aminabhavi, Synergetic degradation of atenolol by  
777 hydrodynamic cavitation coupled with sodium persulfate as zero-waste discharge process: Effect

- 778 of coexisting anions, *Chem. Eng. J.* 416 (2021) 129163. doi:10.1016/J.CEJ.2021.129163.
- 779 [76] M.I. Stefan, J.R. Bolton, Mechanism of the Degradation of 1,4-Dioxane in Dilute Aqueous  
780 Solution Using the UV/Hydrogen Peroxide Process, *Environ. Sci. Technol.* 32 (1998) 1588–1595.  
781 doi:10.1021/es970633m.
- 782 [77] H. Barndök, D. Hermosilla, C. Han, D.D. Dionysiou, C. Negro, Á. Blanco, Degradation of 1,4-  
783 dioxane from industrial wastewater by solar photocatalysis using immobilized NF-TiO<sub>2</sub> composite  
784 with monodisperse TiO<sub>2</sub> nanoparticles, *Appl. Catal. B Environ.* 180 (2016) 44–52.  
785 doi:10.1016/J.APCATB.2015.06.015.
- 786 [78] B. Li, J. Zhu, Simultaneous degradation of 1,1,1-trichloroethane and solvent stabilizer 1,4-dioxane  
787 by a sono-activated persulfate process, *Chem. Eng. J.* 284 (2016) 750–763.  
788 doi:10.1016/j.cej.2015.08.153.
- 789 [79] E. Cako, Z. Wang, R. Castro-Muñoz, M.P. Rayaroth, G. Boczka, Cavitation based cleaner  
790 technologies for biodiesel production and processing of hydrocarbon streams: A perspective on  
791 key fundamentals, missing process data and economic feasibility – A review, *Ultrason. Sonochem.*  
792 88 (2022) 106081. doi:https://doi.org/10.1016/j.ultsonch.2022.106081.
- 793 [80] J.R. Bolton, K.G. Bircher, W. Tumas, C.A. Tolman, Figures-of-Merit for the Technical  
794 Development and Application of Advanced Oxidation Processes, 1 (1996) 13–17.  
795 doi:doi:10.1515/jaots-1996-0104.
- 796 [81] N. Wardenier, Z. Liu, A. Nikiforov, S.W.H. Van Hulle, C. Leys, Micropollutant elimination by  
797 O<sub>3</sub>, UV and plasma-based AOPs: An evaluation of treatment and energy costs, *Chemosphere.* 234  
798 (2019) 715–724. doi:10.1016/J.CHEMOSPHERE.2019.06.033.
- 799 [82] H. Wang, J. Zhan, L. Gao, G. Yu, S. Komarneni, Y. Wang, Kinetics and mechanism of  
800 thiamethoxam abatement by ozonation and ozone-based advanced oxidation processes, *J. Hazard.*  
801 *Mater.* 390 (2020) 122180. doi:10.1016/J.JHAZMAT.2020.122180.
- 802 [83] H. Wang, S. Yuan, J. Zhan, Y. Wang, G. Yu, S. Deng, J. Huang, B. Wang, Mechanisms of  
803 enhanced total organic carbon elimination from oxalic acid solutions by electro-peroxone process,  
804 *Water Res.* 80 (2015) 20–29. doi:10.1016/J.WATRES.2015.05.024.
- 805 [84] Y. Li, D. Wang, G. Yang, X. Yuan, L. Yuan, Z. Li, Q. Xu, X. Liu, Q. Yang, W. Tang, L. Jiang, H.  
806 Li, Q. Wang, B. Ni, In-depth research on percarbonate expediting zero-valent iron corrosion for

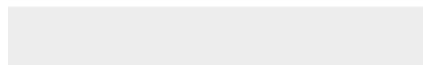
807 conditioning anaerobically digested sludge, *J. Hazard. Mater.* 419 (2021) 126389.  
808 doi:<https://doi.org/10.1016/j.jhazmat.2021.126389>.  
809 [85] A. Fernandes, M. Gągol, P. Makoś, J.A. Khan, G. Boczka, Integrated photocatalytic advanced  
810 oxidation system (TiO<sub>2</sub>/UV/O<sub>3</sub>/H<sub>2</sub>O<sub>2</sub>) for degradation of volatile organic compounds, *Sep. Purif.*  
811 *Technol.* 224 (2019) 1–14. doi:<https://doi.org/10.1016/j.seppur.2019.05.012>.  
812



[Click here to access/download](#)

**Supplementary Material**

Supplementary data of HC-SPC-O3 for CEJ 14 DEC.pdf



**Declaration of interests**

The authors declare that they have no known competing financial interests or personal relationships that could have appeared to influence the work reported in this paper.

The authors declare the following financial interests/personal relationships which may be considered as potential competing interests: